THESIS FOR THE DEGREE OF DOCTOR OF PHILOSOPHY

Controlling the Fluorescence Properties of Diarylethene-based Photochromic Systems

Gaowa Naren

Department of Chemistry and Chemical Engineering

CHALMERS UNIVERSITY OF TECHNOLOGY

Gothenburg, Sweden 2022

Controlling the Fluorescence Properties of Diarylethene-based Photochromic Systems
GAOWA NAREN
ISBN 978-91-7905-626-1

Doktorsavhandlingar vid Chalmers tekniska högskola
Ny serie nr 5092
ISSN 0346-718X

Department of Chemistry and Chemical Engineering
Chalmers University of Technology
SE-412 96 Gothenburg
Sweden
Telephone + 46 (0)31-772 1000

Cover: Illustration of photonically controlled diarylethene-based photochromic systems.

Printed by Chalmers digitaltryck
Gothenburg, Sweden 2022

Controlling the Fluorescence Properties of Diarylethene-based Photochromic Systems

Gaowa Naren

Department of Chemistry and Chemical Engineering

Chalmers University of Technology

Abstract

Diarylethene (DAE) photoswitches are one of the most promising families of photochromic molecules because of their outstanding photophysical/photochemical properties. This class of compounds, which can photoisomerize between an open colorless and a closed colored form, has been applied in various fields in this thesis work, spanning one-color fluorescence intensity modulation, all-photonic full-color reproduction, light-induced color changes for molecular logic gates and information processing. Particularly, all systems presented can be all-photonically controlled, which is extremely beneficial as light is a sustainable resource from nature that is non-invasive, clean, and waste free that also allows for remote operation.

The first part of the thesis deals with introducing the light-induced isomerization process of the diarylethene derivatives. Through the isomerization of DAEs, intrinsic one-color "on-off" fluorescent intensity modulation as well as dynamic multicolor changes can be realized in the designed systems. In paper I, the diarylethene derivative Dasy is applied as a fluorescent probe aiming at phase-sensitive (lock-in) detection for high-contrast cell studies using fluorescence microscopy. The rapid switching fluorescence signal of Dasy can be successfully discriminated from strong fluorescence background using amplitude modulated red light. In paper II, a photoswitch cocktail mixture is designed where the color of the system can be tuned dynamically only by light-controlled isomerizations of the two monomer photoswitches.

The second part of the thesis focuses on discussing Förster Resonance Energy Transfer (FRET) based photoswitching systems where the emission is controlled through FRET processes by harnessing the different absorption and emission properties of the open and closed isomers of the DAE derivatives. In paper III, the FRET process can be orthogonally controlled by selective isomerization of two individual DAE acceptors, which results in an all-photonic full color red-green-blue (RGB) emissive system. In paper IV, a photoswitch triad is used as a sequential molecular logic gate where the emission output can be controlled by two mechanisms, both inherent and FRET controlled intensity change.

Keywords: photochromic molecules, diarylethene, isomerization, FRET, all-photonic, intensity modulation, color change, RGB, molecular logic

List of publications

This thesis is based on the work presented in the following papers:

Paper I

Rapid amplitude-modulation of a diarylethene photoswitch: en route to contrast-enhanced fluorescence imaging

Gaowa Naren,‡ Wera Larsson,‡ Carlos Benitez-Martin, Shiming Li, Ezequiel Pérez-Inestrosa, Bo Albinsson and Joakim Andréasson

Chem. Sci., **2021**, *12*, 7073-7078

Paper II

A simplicity-guided cocktail approach toward multicolor fluorescent systems

Gaowa Naren, Shiming Li and Joakim Andréasson

Chem. Commun., **2020**, *56*, 3377-3380

Paper III

An all-photonic full color RGB system based on molecular photoswitches

Gaowa Naren, Chien-Wei Hsu, Shiming Li, Masakazu Morimoto, Sicheng Tang, Jordi Hernando, Gonzalo Guirado, Masahiro Irie, Françisco M. Raymo, Henrik Sundén and Joakim Andréasson

Nat. Commun., **2019**,*10*, 3996

Paper IV

One-time password generation and two-factor authentication using molecules and light

Gaowa Naren, Shiming Li and Joakim Andréasson

ChemPhysChem., **2017**, *18*, 1726-1729

‡ These authors contributed equally

Publications not included in the thesis

A) *Building pH sensors into paper-based small-molecular logic systems for very simple detection of edges of objects*

Jue Ling, **Gaowa Naren**, Jessica Kelly, Thomas S. Moody and A. Prasanna de Silva

J. Am. Chem. Soc., **2015**, *137*, 3763 – 3766

B) *Small molecular logic systems can draw the outlines of objects via edge visualization*

Jue Ling, **Gaowa Naren**, Jessica Kelly, David B. Fox and A. Prasanna de Silva

Chem. Sci., **2015**, *6*, 4472 – 4478

C) *Fluorescent logic systems for sensing and molecular computation: structure–activity relationships in edge detection*

Jue Ling, **Gaowa Naren**, Jessica Kelly, Adam Qureshi and A. Prasanna de Silva

Faraday Disc., **2015**, *185*, 337 – 346

D) *Measuring electromotance and relationship of original battery potential and temperature by high impedance method*

Jiangchuang Song, Huiling Zhao, Shuran Ma, **Gaowa Naren**, Chuanlin Wang

Power Technology, **2013**, *37*, 2182 – 2184

Contribution report

Description of my contribution to the appended papers:

Paper I

Planned, designed, and evaluated experiments together with W.L. Performed the spectroscopic experiments and analyzed data with W.L. Wrote parts of the manuscript. First authorship shared with W.L.

All synthesis related work is done by S.L. and microscopy measurements are done by C.B.M.

Paper II

Planned and performed all spectroscopic experiments, took part in the design of the system, analyzed the data and drafted the manuscript.

All synthesis related work is done by S.L.

Paper III

Performed all the spectroscopic experiments, optimized the system's performance, evaluated the experimental results and drafted the manuscript.

All synthesis related work is done by C-W. H., S.L., M. M., and S. T.

Paper IV

Performed all the spectroscopic experiments and interpreted all the spectroscopic data.
All synthesis related work is done by S.L.

Table of Contents

1 Introduction 1

2 Fundamentals 5

2.1 Light and matter 5

2.2 Fluorescence 8

2.3 Förster resonance energy transfer (FRET) 10

2.4 Commission of Internationale d'Eclairage (CIE) 12

3 Spectroscopic Techniques 15

3.1 Steady-state absorption spectroscopy 15

3.2 Steady-state fluorescence spectroscopy 17

3.3 Time-correlated single photon counting (TCSPC) 18

4 Photochromic Molecules 19

4.1 Photoisomerization 20

4.2 Fluorescence quantum yield 23

4.3 Diarylethene molecular photoswitches 24

5 Intensity Modulation through Photoinduced Isomerization 27

5.1 Single-color fluorescence photoswitching : turn-off mode fluorescent DAEs 27

5.2 Single-color fluorescence photoswitching : turn-on mode fluorescent DAEs 34

5.3 Multi-color switching of a molecular cocktail 36

6 Intensity Modulation through FRET/PET Process 43

6.1 Emission color tuning by FRET process 47

6.2 Multi-color tunable RGB molecular system 50

6.3 Molecular logic 59

7 Concluding Remarks and Outlook 65

8 Acknowledgements 67

9 References 68

1. Introduction

Photochromic molecules are compounds that can undergo reversible color and structural changes upon photonic stimuli. This class of molecules was first reported in 1867 by Fritzsche who noticed that the color of a tetracene solution was bleached by daylight and regenerated in the darkness.[1] In 1950, Hirshberg named the phenomenon as "photochromism" that comes from two Greek words: *phos* (light) and *chroma* (color), which indicates the light-induced color change.[2]

Actually, except for color and structural changes, many other properties are also altered during the process, such as fluorescent properties, redox energies, and dipole moments.[3,4] Because of distinct characteristics of the two isomers, photochromic molecules are highly interesting and desirable to be applied in various research fields such as photopharmacology,[5-7] fluorescence labeling and bioimaging,[8-15] super-resolution fluorescence microscopy,[16-23] full-color reproduction,[24-28] molecular logic and information storage.[29-35] Photochromic products are also commonly applied in our daily life, such as ophthalmic lenses, security inks, textiles, and cosmetics.[9,36]

In most applications, it is desirable to use photochromic molecules that have distinct emission properties of the two photochromic forms, as the emission intensity or the color of the system can be altered by switching between the two isomers. There are different approaches to modulate the fluorescence of the system, one of the simplest ways is to use a molecular photoswitch monomer that exhibits intense fluorescence in one isomeric form, low or no fluorescence in the other form, as well as efficient photochromism at the same time.[37] In this way, the fluorescent intensity of the system can be easily changed by photoinduced isomerization alone. Inherent fluorescence changes can be found for many photochromic families such as diarylethenes,[38] spiropyrans[39] and fulgimides.[40]

Among different kinds of photochromic molecules, the diarylethenes (DAE) are one of the most promising photochromic families because of their good thermal stability and high fatigue resistance.[4,25,41-43] For many DAE derivatives, it is also possible to enrich the two isomeric forms to virtually 100 % by photoisomerization, which is preferable for the intensity modulation as the fluorescence can be switched between "on" and "off" completely. The "on-off" switching can be used in many areas of applications.[42,44-47] For example, to distinguish the probe signal from autofluorescence background of e.g. a cell in fluorescence microscopy,[48,49]

the fluorescence of a photoswitch can be modulated between two different states with certain frequency, the signal of which can be identified by lock-in amplifier to eliminate the disturbance of cell emission background, which is beneficial for cell studies.[49]

However, the single color "on-off" switching can only provide limited information as there are only two states that can be generated (dark or emissive). In contrast, multi-color fluorescent systems have the advantage to provide various states by including more than one emitting species in the system. For example, by mixing two different DAE derivatives in a solution as a cocktail mixture, the fluorescent color of the system can be gradually changed by photoinduced isomerization.[50] Through light irradiation, the emission color of one photoswitch is turned "off", at the same time the emission of another one is turned "on", which leads to a dynamic color change of the system in a cocktail mixture.

Although the fluorescence can be switched intrinsically by photoinduced isomerization, it is more common to modulate fluorescence by Förster resonance energy transfer (FRET). In this approach, a photoswitch is combined with a fluorophore so that the system allows for an efficient photochromic reactivity and a bright fluorescence simultaneously. Compared to the intrinsic approach (photoisomerization of a monomer photoswitch), it is easier for FRET to offer more desired emission readout as common fluorophores typically have higher emission quantum yields than photochromic molecules.[42] In the FRET process, fluorophores are generally applied as the energy donor and photochromic molecules are used as FRET acceptors. The fluorescence of the system is modulated through the "on-off" switching of the FRET reaction, as the overlap integral between emission of donor and absorbance of acceptor is altered through the isomerization process. However, in this "on-off" switching mechanism, it is not possible to tune the florescent color of the system as the photochromic acceptors typically do not display bright emission subsequent to the FRET reaction.

In 2011, the low inherent fluorescence quantum yields of DAE derivatives were overcome by Irie through the development of DAE sulfones which have fluorescent quantum yields of up to 0.88.[38] The fluorescent closed isomers of the DAE sulfones offer an opportunity to emit intense fluorescence after being sensitized as the FRET acceptor, which achieves emission color tuning of the system concomitant to the isomerization process. In addition, by applying two different photoswitchable DAE acceptors in the system, it is possible to generate full color red–green–blue (RGB) switching through selective isomerization of the two photochromic acceptors and orthogonally controlled FRET reactions.[24]

The work presented in this thesis involves all-optical control of the fluorescent properties of diarylethene-based systems through intrinsic photochromic isomerization and modulation of FRET processes. In paper I, the fluorescence intensity of the DAE derivative Dasy is modulated "inherently" through photoisomerization processes triggered by UV light and modulated red light with various frequencies, the signal of which is easily distinguished from a constant fluorescent background. In paper II, two types of DAE derivatives, Dasy and DAE9 are simply mixed in acetonitrile as a cocktail mixture, the color of which can be dynamically tuned by light-induced isomerization without relying on FRET or other excited state communication reactions. The emission of the system is simply changed in a color-correlated version by all-photonic control. In Paper III, photochromic molecules DAEr and DAEg are applied as FRET acceptors in the tri-component RGB emitting system. Here, the blue emitter perylene acts as the energy donor. The open forms of DAEg and DAEr can be selectively isomerized to the closed isomers, which have emission colors of green and red, respectively. Once DAEg or DAEr is converted to the closed isomer, the FRET process is initiated between the perylene donor and the isomerized photoswitch acceptor. Thus, the overall emission color of the system can be changed continuously from the blue donor emission color to the closed form photoswitch emission (green and red). In Paper IV, the first example of one-time password (OTP) generation and two-factor authentication (2FA) using a molecular approach is reported. The sequential molecular logic is designed with a molecular triad consisting of two fulgimide (FG) and one dithienylethene (DTE) photoswitches. The function of the system relies on two mechanisms, not only by inherent isomerization of photoswitch but also by FRET controlled intensity change.

To summarize, although the applications mentioned above span a relatively large area, the underlying fundamental principle is the same: all-photonic control of the emission properties of photochromic systems. As indicated above, and which will also become apparent throughout this thesis, this control can be achieved in several fundamentally different ways, and the resulting emission changes span from trivial one-color "on-off" to much more complex multi-color continuous changes. Speculations on potential future applications left aside, the ability to precisely predict and control the emission properties of molecular systems is both exciting and fundamentally important, and this is what the thesis is all about.

2. Fundamentals

2.1 Light and matter

Light can be described as an electromagnetic radiation that includes near-infrared (wavelength region around 700–1400 nm), visible (can be perceived by human eyes with wavelengths in the range of around 400–700 nm) and ultraviolet regions (wavelength region around 100–400 nm). The electromagnetic radiation is a wave of electric and magnetic fields that oscillate perpendicular to each other as illustrated in Fig.2.1. The distance between two periodical waves is defined as the wavelength of light, λ.

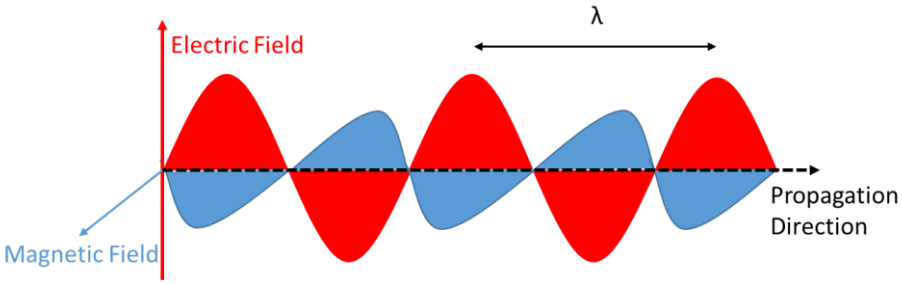

Figure 2.1. Schematic illustration of light as an electromagnetic wave.

Due to the wave-particle duality, light can be considered not only as electromagnetic waves, but also as particles called photons. In Planck's equation, the light can thus also be regarded as a flow of photons, the energy of a photon E being proportional to the respective frequency of oscillation v:

$$E_{photon} = hv \qquad (2.1)$$

where h is Planck's constant ($h = 6.63 * 10^{-34}\ Js$). The frequency v and the wavelength λ are related as:

$$\lambda = c/v \qquad (2.2)$$

where $c = 2.98 * 10^{8}\ ms^{-1}$ is the speed of light.

In the interaction of light with matter, if the energy of light is the same as energy difference of the initial and final state, the photon can be absorbed or emitted by the molecule. It is described

by the Bohr frequency condition shown in equation (2.3) where ΔE is the energy difference between the final state (E_{final}) and the initially state ($E_{initial}$), h is Planck's constant and v is the frequency of the light.

$$\Delta E = E_{final} - E_{initial} = hv \quad (2.3)$$

When a photon is absorbed by a molecule (referred to as M), the molecule is excited from the ground state to the excited state M^*:

$$M + hv_1 \rightarrow M^* \quad (2.4)$$

Several processes can happen after the molecule has been excited, which can be seen in the Jabłonski diagram shown in Fig.2.2, S_0 stands for the electronic ground state and S_1, S_2 stand for singlet electronically excited states. There are several vibrational energy levels shown as 0, 1, 2… at each electronic energy level.

Based on the Franck-Condon principle, electronic transitions are much faster than the nuclear motion, which results in so-called vertical transitions, that is, the positions of nuclei do not change during excitation. Usually, after excitation, the molecule will start to relax to the lowest vibrational energy level of S_1 from the higher electronic and vibrational level by internal conversion (IC) and vibrational relaxation (VR). The time scale of relaxation is around 10^{-12} s or less, which is typically much faster than processes depopulating S_1.

Once a molecule reaches the lowest vibrational level of S_1, different processes can happen. There are non-radiative processes, such as internal conversion (IC) and intersystem crossing (ISC), which are competing with the radiative process (fluorescence). IC brings the molecule back to the ground state S_0 while ISC brings the molecule to a triplet excited state (here T_1). The spin state of the excited molecule is changed by ISC when moving to a triplet excited state. From T_1, the process can be followed by non-radiative relaxation or phosphorescence, which is a radiative process. It is a long-lived emission compared to fluorescence as the transition from T_1 to S_0 is spin-forbidden.

The radiative process from S_1 to S_0 is referred to as fluorescence. The process will be further discussed in the next section. Molecules that revert to the ground state by mainly the fluorescent channel are referred to as fluorophores.

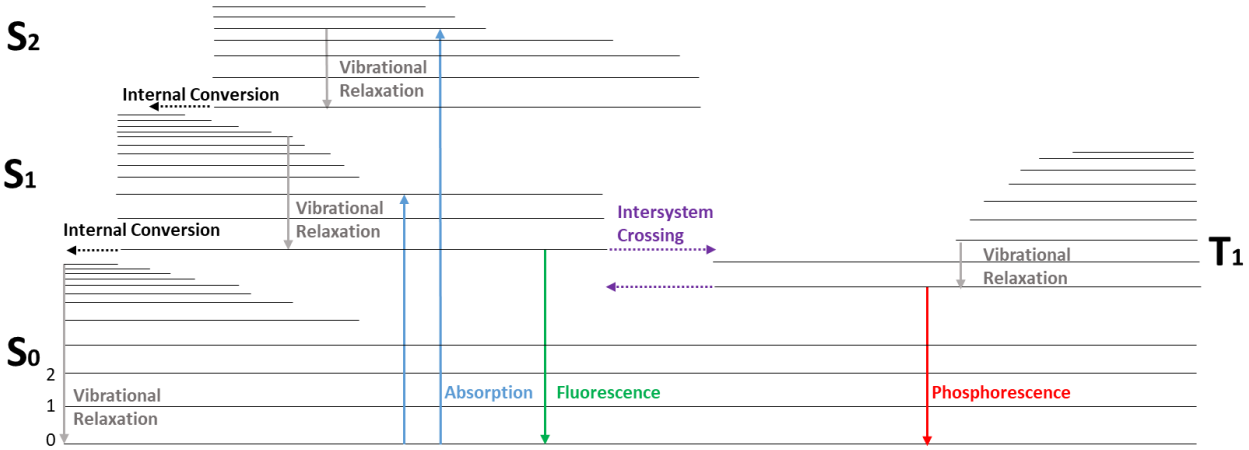

Figure 2.2. Jabłonski diagram indicating the non-radiative and radiative processes after a molecule is excited.

2.2 Fluorescence

The emission process can be shown as the reaction below:

$$M^* \rightarrow M + h\nu_2 \qquad (2.5)$$

The emission of light can be divided into fluorescence and phosphorescence depending on different nature of excited states. The process is known as phosphorescence if the photonic energy released is from a triplet excited state to the singlet ground state (or rarer, from a singlet excited state to a triplet ground-state). If the photon is emitted in a process involving singlet states only, the process is referred to as fluorescence. Based on Kasha's rule and described above, generally, the fluorescence is emitted from the lowest vibrational level of the first excited electronic state S_1. The fluorescence emission process is spin-allowed, implying that fluorescence lifetimes are typically much shorter (on the ns timescale) compared to phosphorescence (ms to s timescale).

The fluorescence occurs at longer wavelength compared to the absorbance. This is due to the rapid vibrational relaxation processes to the lowest vibrational level of S_1 before depopulation occurs. Another reason for the observed redshift of the emission is solvent reorganization. The solvent dipole can reorient or relax around the molecular dipole in the excited state (μ_E) which is typically larger (and differently oriented) than the dipole moment in the ground state (μ_G).[51] In solution, solvent relaxation happens in a time range between 10–100 ps at room temperature. This means that compared to the emission process, which happens typically occurs in 1–10 ns, the absorption of light (about 10^{-15} s) is too fast for fluorophore or solvent to have any motion during that time range.

There are two important parameters for describing the excited state deactivation by fluorescence: *fluorescence quantum yield* and *fluorescence lifetime*. The fluorescence quantum yield is defined as the ratio between the number of photons emitted by the fluorophore and the number of photons absorbed by the same molecule, as indicated in equation (2.6):

$$\Phi = \frac{No.\ of\ emitted\ photons}{No.\ of\ absorbed\ photons} \qquad (2.6)$$

The fluorescence quantum yield can be calculated by the ratio of rate constants:

$$\Phi = \frac{\Gamma}{\Gamma + k_{nr}} \qquad (2.7)$$

Where Γ stands for the fluorescence rate constant and k_{nr} stands for rate constant of non-radiative decay processes (typically $k_{isc} + k_{ic}$).

The fluorescence lifetime is a measure on the average time a molecule spends in the excited state before relaxing back to the ground state. It is an important property of a fluorophore that gives information about the availability of the fluorophore interacting with its environment while being excited. As indicated above, the fluorescence lifetimes are typically in the ns timescale. The relation between lifetime and rate constants is shown in equation (2.8).

$$\tau = \frac{1}{\Gamma + k_{nr}} \qquad (2.8)$$

2.3 Förster resonance energy transfer (FRET)

The molecule may depopulate from the excited state also by transferring its excitation energy to a nearby molecule. This process can be described as the energy transfer shown in equation (2.9) where the energy of the excited donor (D^*) is transferred to the acceptor in the ground state (A) without appearance of a photon. There are two types of energy transfer interactions: Förster and Dexter transfer. Förster resonance energy transfer (FRET) is a through space interaction, which means the energy can be transferred by long range dipole–dipole interactions between the donor and the acceptor. In contrast, the Dexter mechanism requires the donor and acceptor at contact distance and the process is governed by a double electron exchange process. This mechanism, however, is not expected to be of any major importance in the work conducted in this thesis and will not be further elaborated on here.

$$D^* + A \rightarrow D + A^* \qquad (2.9)$$

For FRET to occur, there must be a spectral overlap between the emission of the donor and the absorbance of the acceptor, and a sufficient proximity between the donor and the acceptor as well. The equation of FRET rate between a donor and an acceptor is shown in equation (2.10).

$$k_T(r) = \frac{\phi_D \kappa^2}{\tau_D r^6} \left(\frac{9000(ln10)}{128\pi^5 N n^4}\right) J \qquad (2.10)$$

It can be seen that rate is influenced by many factors: spectral overlap between donor and acceptor J, the ratio of the fluorescence quantum yield ϕ_D and the fluorescence lifetime τ_D of donor (which equals the rate constant of fluorescence of the donor), the relative orientation between the donor and the acceptor dipole moments κ^2 (generally assumed to be 2/3, which is the average orientation of freely rotating molecules), the separation distance between donor and acceptor r (to the power of 6, showing how strongly dependent on distance this process is), and the refractive index n of the intervening medium (typically the solvent used).

The spectral overlap J can be calculated by equation (2.11) where $F_D(\lambda)$ is the area normalized emission spectrum of the donor and $\varepsilon_A(\lambda)$ is the wavelength-dependent molar absorption coefficient of the acceptor.

$$J = \int F_D(\lambda) * \varepsilon_A(\lambda) * \lambda^4 d\lambda \qquad (2.11)$$

The FRET interaction can be described by the Förster distance R_0 that is defined as the distance between donor and acceptor when the FRET efficiency is 50%. The energy transfer efficiency E_T can be expressed by R_0 and r:

$$E_T = \frac{{R_0}^6}{{R_0}^6 + r^6} \tag{2.12}$$

The energy transfer efficiency can also be measured by comparing the fluorescence intensity of the donor without acceptor F_D and in the presence of acceptor F_{DA} as equation (2.13) shows.

$$E_T = 1 - \frac{F_{DA}}{F_D} \tag{2.13}$$

Another way to calculate the energy transfer efficiency is to measure the lifetimes of donor under respective conditions (τ_{DA} and τ_D):

$$E_T = 1 - \frac{\tau_{DA}}{\tau_D} \tag{2.14}$$

2.4 Commission of Internationale d'Eclairage (CIE)

As the emission from a fluorophore spans a range of wavelengths, it is not possible to intuitively judge the emission color of the fluorophore by looking at the emission spectrum only. In 1931, the system named as "CIE 1931 color space" was designed by the Commission of Internationale d'Eclairage (CIE), which is the first system that relates the distribution of photon energies in an electromagnetic spectrum to the perceived colors in human color vision.[52]

The system defined the standard observer that represent an average chromatic response of human eyes. As seen in Fig.2.3,[53] $\bar{x}, \bar{y}, \bar{z}$ stand for the spectral sensitivity curves of the observer to three primary colors red, green, and blue respectively.[52] The spectral overlap integrals between a given fluorescence spectrum and $\bar{x}, \bar{y}, \bar{z}$ are calculated by equations (2.15a-c). The calculated overlap integrals values X, Y and Z stand for contributions of the spectrum to each of the three primary colors red, green, and blue, respectively.

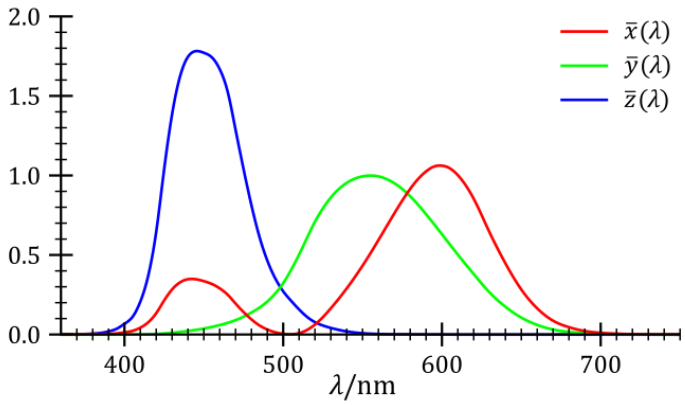

Figure 2.3. The CIE XYZ standard observer of three primary colors red ($\bar{x}$), green ($\bar{y}$), and blue ($\bar{z}$).[53]

$$X = \int_0^\infty I(\lambda)\bar{x}(\lambda)d\lambda \qquad (2.15a)$$

$$Y = \int_0^\infty I(\lambda)\bar{y}(\lambda)d\lambda \qquad (2.15b)$$

$$Z = \int_0^\infty I(\lambda)\bar{z}(\lambda)d\lambda \qquad (2.15c)$$

The CIE coordinates are then calculated based on equations (2.16) and mapped in CIE diagram as shown in Fig.2.4. The location of the coordinates in CIE diagram gives the result of the perceived color of the molecule emission.

$$x = \frac{X}{X+Y+Z} \qquad y = \frac{Y}{X+Y+Z} \qquad z = \frac{Z}{X+Y+Z} \qquad (2.16)$$

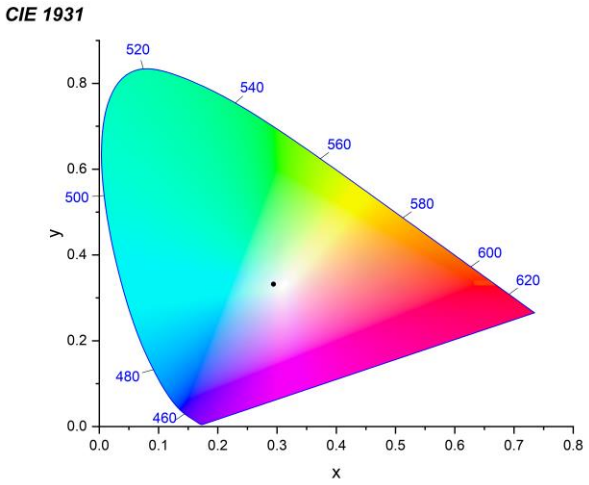

Figure 2.4. The CIE 1931 color space chromaticity diagram with an arbitrarily mapped coordinates (x,y).

3. Spectroscopic Techniques

3.1 Steady-state absorption spectroscopy

The process where a molecule absorbs light energy when being exposed to photons is referred to as absorption. The absorption process can be studied by using UV-vis absorption spectroscopy as shown in Fig.3.1.

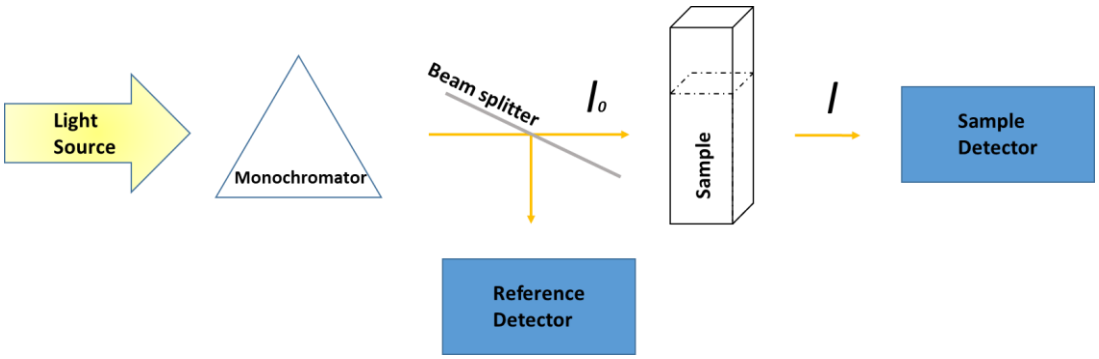

Figure 3.1. Schematic setup of a UV-vis absorption spectroscopy.

In the measurement, white light passes through a monochromator and then split up into two beams: one beam is used as the reference with the detected intensity I_0; another beam is passed through the sample and the transmitted intensity I is measured by the detector. According to Lambert Beer's law, the absorption A can be calculated by the logarithm of ratio between transmitted light I and the incident light I_0 as shown in equation (3.1).

$$A = log \frac{I_0}{I} = \varepsilon cl \qquad (3.1)$$

where c is the concentration of the absorbing molecule in the sample (in M) and l is the path length of light (in cm) and ε is the molar absorption coefficient (in $M^{-1}cm^{-1}$). The molar absorption coefficient gives information about the ability of a molecule to absorb light at a specific wavelength. The shapes of the absorption spectra are determined by the wavelength dependence of the molar absorption coefficient.

Absorption spectroscopy can be used to determine the molar absorption coefficient with a known concentration or can be used to calculate the concentration of a sample when the extinction coefficient is known. Moreover, the technique is often used to study how fast

reactions proceed (kinetics), given that the timescale of the reaction is on the order of seconds or slower. For photochromic molecules, it is also very convenient to use absorption spectroscopy to determine the optimal isomerization wavelength (see paper II and paper III).

3.2 Steady-state emission spectroscopy

The steady state emission and excitation spectrum of a sample can be recorded by a spectrofluorometer. The experimental setup is shown in Fig.3.2.

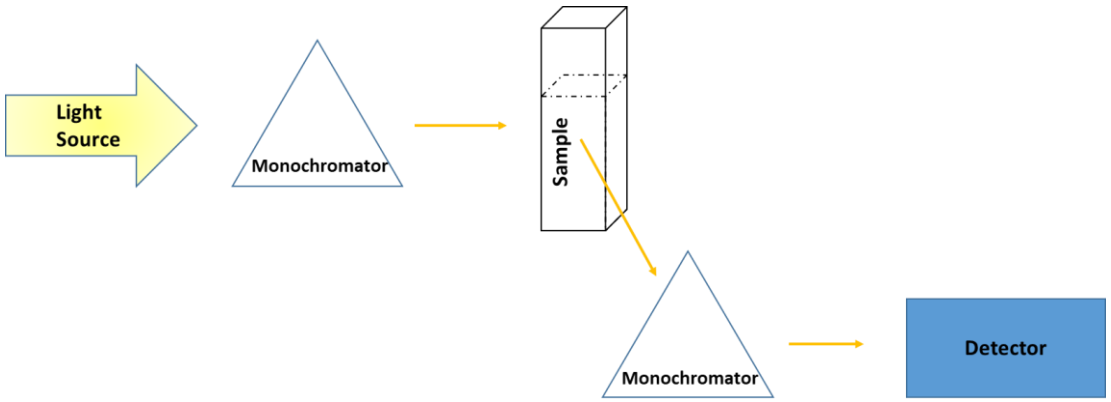

Figure 3.2. Schematic basic setup of steady-state emission spectroscopy.

When the instrument is used to measure the emission spectrum, a specific excitation wavelength is selected to excite the sample. The emission from the sample in a chosen wavelength region is scanned by the emission monochromator. This measurement reveals the emission properties of the sample.

In contrast, when the instrument is used to measure the excitation spectrum, the emission wavelength is fixed while the excitation light is scanned through the absorption range. This type of measurement is used to investigate which wavelengths of excitation light are contributed to the emission of the selected wavelength.

The instrument can also be used for kinetic studies to record changes in fluorescence intensity as a function of time when the sample is irritated at a fixed wavelength. Fluorescence detection is highly sensitive, which is why this technique is preferred over absorption spectroscopy for dilute samples or small molecular ensembles.

3.3 Time-correlated single photon counting (TCSPC)

Time-correlated single photon counting is used to measure the fluorescence lifetime of a sample, investigating how its emission decays with time. After the sample is excited by e.g. a laser pulse, the intensity of the photons emitted by the sample decays typically exponentially with time (at least for a homogeneous sample). For TCSPC, the time interval between the excitation pulse and the first detected photon is recorded. By repeating the excitation process, the histogram of emitted photons is recorded, which represents the emission decay of the sample. The measurement generally needs to collect enough photons (5000 or 10000 in the top channel) to build a desired emission intensity decay. Typically, low counting rate 1% (one photon detected for every 100 excitation pulses) is applied for TCSPC to avoid pulse pileup (the apparent decay becomes non-exponential).

As the excitation pulse is also measured by the detector, the measured decay curve is a convolution between instrument response function (IRF) and emission decay of the sample. To calculate the emission lifetime, instrument response function (IRF) needs to be deconvoluted from the measured decay curve to get the true fluorescence decay.

The fluorescence intensity I of a molecule follows the equation (3.2) where I_0 is the initial intensity, t is the time taken after excitation and τ is the measured fluorescence lifetime.

$$I(t) = I_0 e^{-t/\tau} \qquad (3.2)$$

For systems containing more than one emission species, a multi-exponential decay can be applied as shown in equation (3.3) where α is the amplitude of different species and n is the number of different species.

$$I(t) = \sum_{i=1}^{n} \alpha_i \, e^{-t/\tau} \qquad (3.3)$$

TCSPC measurements can provide information which cannot be obtained from steady-state data. For example, it can distinguish if the quenching of the system is static or dynamic by measuring the lifetime. In addition, the FRET efficiency can be calculated by knowing the lifetime of a donor-acceptor pair, based on equation (2.14).

4. Photochromic Molecules

The word “Photochromism” comes from “*phos*” and “*chroma*”, which are two Greek words meaning light and color, respectively.[1] Photochromic molecules display reversible structural and color transformations upon isomerization. Generally, the isomerization processes can be triggered by light at different wavelengths. In effect, color changes occur as a result of structural changes. In addition to the color and the structural changes, there are many other properties that also change between the different isomers, such as fluorescent properties, redox energies, dipole moments, refractive index and so on.[3,4] In principle, a good rule is to assume that almost every molecular property is changing upon isomerization between the two states.

The first example of a photochromic molecule was documented in the late 19th century.[2] Nowadays, there are a large number of different types of photoswitchable molecular families such as diarylethenes, spiropyrans, azobenzenes and fulgimides that have been widely used in various areas of natural science, where the differences in properties between the two isomers are exploited. Especially in the two recent decades, photochromic molecules have shown great potential in many fields, such as in the fabrication of photocontrollable organic field effect transistor (OFET),[54-59] incorporation into metal organic framworks (MOFs),[60-65] super-resolution fluorescence microscopy,[16-23] molecular computing and information storage[36,47,66-73] as well as bioimaging and photocontrollable biological functions.[5-15]

In addition, photochromic materials are also popular in the industry area and those products are commonly seen in our daily life, such as ophthalmic lenses, security inks, textiles, cosmetics, photochromic helmet visors, and interestingly, fishing lines - the line is concealed for fishes as there is insufficient UV penetration below the water surface while the line is obviously visible for anglers as the color of the fish line shows up above the water surface.[9,36]

The main driver for using photochromic molecules is the possibility of the system being all-photonically controlled, which enables the system to respond instantaneously and be manipulated remotely. In addition, it is extremely beneficial to use light as the energy input as it is a sustainable resource from nature that is non-invasive, clean, and waste free. Therefore, it is highly important to study and develop all photonic system based on photochromic molecules, which is the aim and the topic of this thesis.

4.1 Photoisomerization

Photoisomerization of photochromic molecules can be schematically described as the process below.

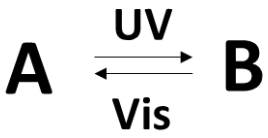

Commonly, the colorless form A is thermodynamically stable and can be transformed to the colored form B by ultraviolet (UV) irradiation. Form B can be isomerized back to A by visible light or thermal activation. During isomerization, chemical bonds are rearranged, typically in the form of cyclization reactions or E/Z transformations. By the differences in thermal reversibility, the photochromic molecules are classified as either P-type or T-type.[74] For P-type photochromic molecules, as they are thermally irreversible, the reversible transformation can only be induced by light irradiation. As for T-type photochromic molecules, in addition to photoinduced isomerization, they are thermally reversible as well. In most cases, the colorless isomer is thermally stable, as opposed to negative photochromism where the colored form displays the highest stability.[75,76] For some applications, thermal stability is desired, such as optical memory media[77], whereas in other applications the opposite is true. Examples are photochromic photoacids, and light-controlled ion channels.[78,79]

The photoisomerization process is schematically described in Fig.4.1 below.[80] After A is excited to the excited state A*, it can be transformed to the isomer B. The isomer B can also be transformed back to the A-form after being excited to B*. There are important parameters used to evaluate the efficiency of photochromic switching: the *isomerization quantum yield* (Φ_{iso}) and the *photostationary distribution* (PSD). For the isomerization process form A to form B, the isomerization quantum yield can be calculated by equation (4.1), the number of generated isomers B compared to the number of photons absorbed by isomer A.

$$\Phi_{A-B} = \frac{No.\ of\ B\ isomers\ generated}{No.\ of\ absorbed\ photons\ by\ A} \qquad (4.1)$$

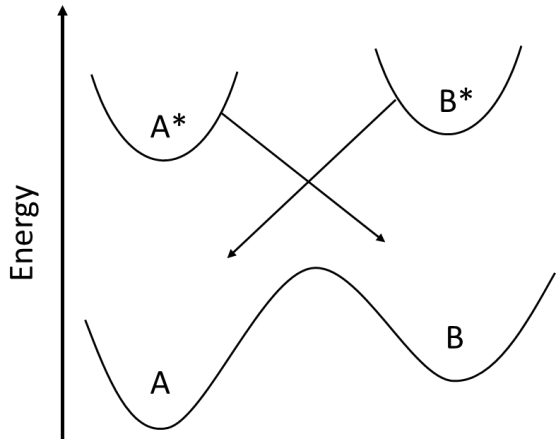

Figure 4.1. The light-induced isomerization by light (arrows) between two isomers, A and B.

The isomerization rate constant from A to B, $k_{\text{A-B}}$ is proportional to the light intensity I(λ), the molar absorption coefficient $\varepsilon_{\text{A}}(\lambda)$, and the isomerization quantum yield ϕ_{A-B} (neglecting any wavelength dependence of the isomerization quantum yield).

$$k_{\text{A-B}} \propto \text{I}(\lambda)\ \varepsilon_{\text{A}}(\lambda)\ \phi_{A-B} \qquad (4.2)$$

A common way to measure isomerization quantum yields is to compare the kinetics of isomerization of the unknown sample to that of the reference for which the isomerization quantum yield is known. The ratio of isomerization rate constants of the reference and the sample is equal to the ratio of their multiplicative products $I * \Phi * \varepsilon$ (assuming that the light only triggers isomerization in one direction A→B and the thermal isomerization process is slow). In the common case where the same light source is used to trigger the isomerization processes of both reference and the sample, the ratio of their isomerization rate constants is only determined by their ratio of $\Phi * \varepsilon$. Therefore, when knowing the isomerization quantum yield of the reference Φ^r_{A-B}, the absorption coefficient for both sample ε^s_A and the reference ε^r_A at the excitation wavelength, the isomerization quantum yield of the sample Φ^s_{A-B} can be calculated by equations (4.3 and 4.4) below:

$$\frac{k^s_{A-B}}{k^r_{A-B}} = \frac{I*\Phi^s_{A-B}*\varepsilon^s_A}{I*\Phi^r_{A-B}*\varepsilon^r_A} = \frac{\Phi^s_{A-B}*\varepsilon^s_A}{\Phi^r_{A-B}*\varepsilon^r_A} \qquad (4.3)$$

$$\Phi^s_{A-B} = \frac{k^s_{A-B}*\Phi^r_{A-B}*\varepsilon^r_A}{k^r_{A-B}*\varepsilon^s_A} \qquad (4.4)$$

When isomerization rate $r_{A\text{-}B}$ is equal to $r_{B\text{-}A}$, the isomeric composition reaches to the photo-equilibrium that is reflected as the photostationary distribution (PSD). The PSD shows the relative efficiency of the interconversion process for one photochromic isomer to the other. The PSD can be expressed by the equation (4.5).

$$PSD = \frac{[A]}{[B]} = \frac{\Phi_{B-A} * \varepsilon_B}{\Phi_{A-B} * \varepsilon_A} \qquad (4.5)$$

If the isomerization quantum yield is assumed to be independent of irradiation wavelength, the concentration ratio of two forms at the PSD is simply determined by the irradiation wavelength (that is, by the ratio of the molar absorption coefficients at the wavelength used to trigger the isomerization). Please note that all arguments above require that any thermal isomerization process is much slower than the corresponding photoinduced isomerization processes.

4.2 Fluorescence quantum yield

For some fluorescent photoswitches, the emissive behavior can be dramatically altered by the photoinduced isomerization, given that one isomer is non-fluorescent while the other one emits strong fluorescence. Such switching property can be applied to many fields, such as super resolution fluorescence microscopy, optical memories, and logic gates.[42,44-47] Therefore, it is crucial to know the emission property of different fluorescent isomers, which can be evaluated from the fluorescence quantum yield. The fluorescence quantum yield can be calculated by using absorption and emission spectrometers,[81] as shown in the equation (4.6):

$$\Phi_f^i = \frac{F^i f_s n_i^2}{F^s f_i n_s^2} \Phi_f^s \qquad (4.6)$$

Here, Φ_f^i stands for the fluorescence quantum yield of the unknown sample while Φ_f^s stands for the fluorescence quantum yield of the standard. F^i and F^s are the integrated intensities of the fluorescence spectrum of the sample and the standard, respectively. The refractive indices of the solution in sample and reference are n_i and n_s, respectively. f_i and f_s are the absorption factors of sample and reference, respectively. $f = 1 - 10^{-A}$, where A is the absorbance at the excitation wavelength. At very low absorbances (negligible inner filter effect), f may be replaced with the absorbance A.

To make sure the accuracy of the measurement, there are some key points to address. Firstly, it is better to choose the same excitation wavelength for the sample and the reference as the relative photon flux at the two wavelengths can be different. Secondly, the absorbance should be kept as low as possible (while still maintaining a sufficient signal-to-noise ratio) to avoid the inner filter effect and errors from uneven distribution of the excited species in the detection volume. In addition, it is advisable to use a similar emission spectral range and emission intensities for both the unknown sample and reference to reduce errors resulting from imperfect correction of detection system in the fluorimeter. In summary, to minimize errors, the absorption and emission spectra of the standard and the sample should match as closely as possible.

In 2011, IUPAC published standards for photoluminescence quantum yield measurements in solution,[81] which is a very useful guideline for measuring the fluorescence quantum yield. As various standards in different wavelength regions are listed, it serves as a good reference work in the search for suitable standards based on the requirements of the sample.

4.3 Diarylethene molecular photoswitches

The diarylethenes (DAE) belong to the major families of photochromic compounds. Among different kinds of photochromic molecules, the diarylethenes are highly promising because of their good thermal stability and high fatigue resistance.[4,25,41-43] The family of diarylethenes and their derivatives can display a broad range of applications, such as organic field-effect transistors,[57-59] metal organic frameworks,[60-65] super-resolution fluorescence microscopy,[47,82-84] full-color reproduction,[24-28] fluorescence labeling and bioimaging,[85-89] molecular logic and information storage.[29-35]

Diarylethenes exist in an open colorless form (typically absorbing only at wavelengths shorter than 400 nm, although some derivatives display absorption also at longer wavelengths) that is isomerized to the closed colored form by exposure to UV light. By isomerization to the closed form, the "localized" π conjugation of the open isomer is spread over the whole photochromic core, which leads to a shift in the absorbance of the closed form to longer wavelengths. The reverse reaction is triggered by exposure to visible light. One example of diarylethene isomerization is DAE8 shown in Fig.4.2 where DAE8(o) and DAE8(c) stands for the open and closed form of DAE8, respectively.

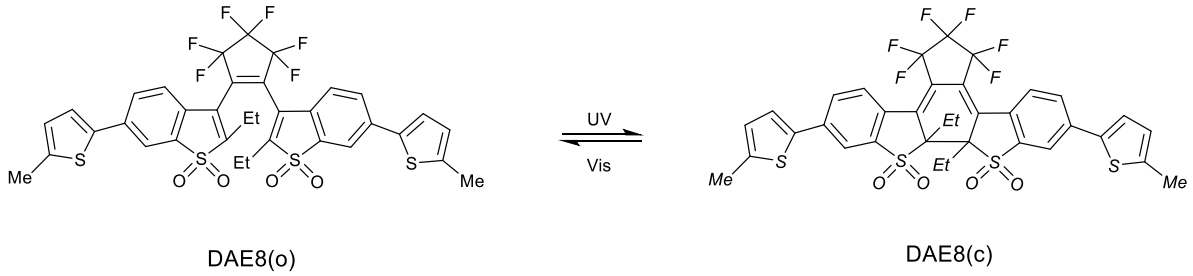

Figure 4.2. The isomerization process of DAE8 between the open form and the closed form.

The open form of a DAE molecule has antiparallel and parallel conformations, which can convert to each other in solution.[4] Typically, the cyclization quantum yield does not exceed 0.5 as the ratio of two conformations is 1:1 in most cases and the allowed conrotatory cyclization reaction only proceeds from the antiparallel conformation.[90] However, it is possible to increase the cyclization quantum yield by introducing bulky substituents[91] or long alkyl groups[92] at the active carbon, which can increase the population of the antiparallel conformation.

The cyclization quantum yield of DAE molecules can be largely influenced by solvent effects because of the formation of internal charge transfer (ICT) states or twisted internal charge transfer (TICT) states.[4,93,94] For example, the fluorescent solvatochromism observed for DAE8 is ascribed to the intramolecular charge-transfer (ICT) between the electron-donating thiophene rings and central electron-accepting benzothiophene 1,1-dioxide groups.[95] The cyclization quantum yield becomes lower with the increased polarity of the solvent. A similar trend of decreased cyclization quantum yield was also seen in other fluorescent diarylethene derivatives containing electron-donating substituents at 6- and 6′-positions of benzothiophene 1,1-dioxide groups.[20,95,96]

Although the open isomer of DAE derivatives is thermodynamically stable, the rate of thermal isomerization from the closed to the open isomer is typically extremely slow. The thermal stability of the closed isomer is influenced by the energy differences between open and closed forms. When the energy difference is small, the thermal cycloreversion reaction is constrained by the large activation energy. For DAE derivatives, the energy difference between the two isomers can be strongly influenced by the choice of aryl group. For aryl groups with low aromatic stabilization energy, such as furyl, thiophene and benzothiophene, there is not much energy lost during the cyclization process so that the closed isomers of DAE derivatives revert very slowly to the open isomer. For phenyl, pyrrolyl, or indolyl aryl groups with high aromatic stabilization energy, there are large energy differences between the open and the closed isomers due to the significant loss of the aromatic stabilization energy.[4,90]

Because of its good thermal stability, the DAE derivatives are therefore classified as P-type photoswitches–enabling photoinduced interconversion while having very slow thermal reversion to the open isomer. In addition, for many DAE derivatives it is possible to enrich the two isomeric forms to virtually 100 % by photoisomerization. This favorable observation results from the fact that typically, the isomerization quantum yield for the cyclization (closing) reaction is much higher compared to the reverse isomerization. Hence, despite the fact that the UV-light used for cyclization is also absorbed by the closed isomer, the cyclization reaction “wins”, and the resulting PSD is highly enriched in the closed form. In combination with the good photostability, this is what makes the DAE photoswitches so broadly applied.

5. Intensity Modulation through Photoinduced Isomerization

5.1 Single-color fluorescence photoswitching: turn-off mode fluorescent DAEs

When photochromic compounds are excited, there is a competition between isomerization, non-radiative internal conversion/intersystem crossing, and radiative decay (fluorescence). For some photochromic molecules, like azobenzene, both isomeric forms are non-fluorescent as the radiative decay is too inefficient to compete with the other deactivation processes. Therefore, it is common to design molecular systems that can combine both fluorescence and photochromic activity by linking fluorescent and photochromic moieties through covalent bonds or using hybrid materials consisting of separate fluorescent and photochromic parts.[37] However, for those systems, much work is typically needed for the tedious synthesis of covalently linked constructs or the formation of supramolecular systems.

In this regard, it is thus more desirable to control the fluorescence intensity only by using a molecular photoswitch monomer that exhibits both intense fluorescence and efficient photochromism. Given that only one of the two isomers displays distinct fluorescence, the emission intensity can be reversibly altered by isomerization between the two forms.

Among all different types of photochromic molecules, there are some compounds that possess inherent fluorescence only in one of the two isomers. The typical DAE derivative is weakly fluorescent in the open isomer, whereas the closed-ring isomer displays no detectable emission.[4,37] Therefore, weak fluorescence is observed in the "initial" open isomeric state and the intensity of the emission decreases by the irradiation of UV light. Typically, the fluorescence quantum yield of the open form of DAEs is very low. Exceptions are rare, but includes one example where the fluorescence quantum yield was reported to be close to 20%.[97] This value was determined in hexane solution and the closed isomer cannot be fully reached upon UV irradiation, implying it is not possible to totally switch ''off'' the emission.

In our projects, the open isomer of Dasy is noticed to have the advantage of reaching virtually 100% closed form by exposure to UV light. The structure and the isomerization scheme for Dasy is shown in Fig.5.1. The fluorescence quantum yields of Dasy open isomer are 0.21 in water[49] and 0.11 in acetonitrile[50], which are extraordinarily high among open isomers of DAE

derivatives. Because of its good water solubility, exceptionally high fluorescence quantum yield, virtually quantitative enrichment in both photostationary states, and robust switching capabilities, Dasy is a very suitable candidate to be applied in rapid fluorescent amplitude modulation, which could be very useful in fluorescence microscopy, as explained in detail below.

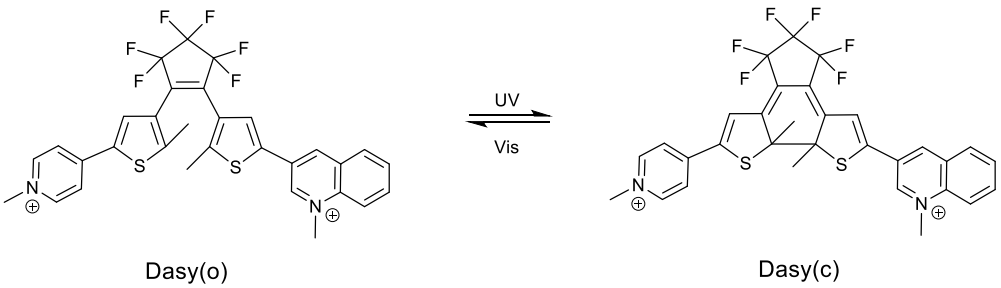

Figure 5.1. The isomerization process of Dasy between the open form and the closed form.

Generally, synthetic fluorescent probes are used in fluorescence microscopy to discriminate between fluorescent and non-fluorescent materials. However, because of the autofluorescence of the cells, the light used to excite a fluorescent probe can also excite interfering background fluorescence. In addition, there is also interference from scattering of the excitation light. As a consequence, the signal to background ratio is limited, which results in the reduction of the contrast.[98-100] Therefore, a major challenge in, e.g., live-cell imaging is to isolate the fluorescent signal of interest from the background. Among different approaches, optical lock-in detection (OLID) is an efficient technique to discriminate the fluorescence signal of probe from the fluorescent background.

By using homodyne detection scheme (extraction of an oscillating signal) and low-pass filtering, a lock-in measurement can extract the amplitude and phase of the signal from noisy background. In OLID, the amplitude-modulated signal (AC component) of a fluorescent probe is "separated" by a lock-in amplifier with respect to the static (DC component) background.[101] The OLID can extract the AC component even when the intensity is 0.1% or less of the total signal.[102] The key to success of the system is therefore depending on the ability of the probe to display rapid, reversible switching between two distinct states in multiple cycles, and, of course, that one isomeric form displays intense fluorescence. The conventional fluorescent probe has limitations as for being applied in lock-in detection, as the modulation of the excitation light will trigger in-phase oscillations of the autofluorescence of the background as well. OLID technique requires a fluorescent probe that can be optically modulated between the

"on" and "off" states to generate a fluorescence intensity waveform that can be defined by the lock-in amplifier from the non-modulated background.[103] The use of photochromic probes in which the emission can be switched by amplitude modulated excitation light has been generated and analyzed for this purpose.

There are several approaches to design photochromic molecules that can be potentially applied in lock-in detection. However, in most cases the photo-controlled FRET process is essential for running the system, which implies that extensive synthesis is required. Typically, the modulation frequency is only 1 Hz or lower which leads to unpractically long acquisition times.[98,99,104,105] Marriott and co-workers have improved the system by using a spiropyran photoswitch as the sole probe in a cellular environment.[100,106] However, the downsides of the poor photostability and very low fluorescence quantum yield of the probe limit its further application in cell imaging. In addition, much data processing is required to separate the probe signal from the background as the spiropyran has fluorescence in its colored form instead of the colorless form.

In our approach, Dasy is successfully applied as the sole fluorescent probe in phase-sensitive (lock-in) detection system where all the downsides mentioned above have been eliminated.[49] We show that the fluorescence of Dasy can be switched rapidly by using amplitude modulated red light, which avoids the disturbance of the background emission as those fluorescent species absorb at wavelengths shorter than red light and the scattered light is in the visible region. Therefore, only the fluorescence signal of Dasy can be modulated and distinguished by the lock-in amplifier. The lock-in detection of Dasy is easily done at frequencies up to 205 Hz, and the method can be applied to cell studies by using fluorescence microscopy. So far there is no other class of photochromic molecules that has intrinsically high fluorescence quantum yield in the colorless form, and hence Dasy is an exceptionally well suited fluorescent photoswitch for this purpose.

The absorption and emission spectra of Dasy are shown in Fig.5.2. It can be seen that the open form of Dasy (Dasy(o)) absorbs mostly in the UV region with its most redshifted absorption band centered at 351 nm in aqueous solution. UV light triggers isomerization from Dasy(o) to virtually 100% (Dasy(c)) at the photostationary state. The closed form of Dasy (Dasy(c)) has its most redshifted absorption band centered around 650 nm in aqueous solution. The emission of Dasy(o) centered around 511 nm in aqueous solution while Dasy(c) is non-fluorescent.

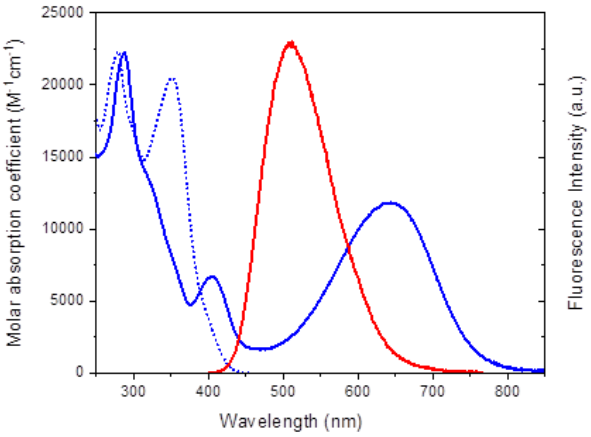

Figure 5.2. The absorption spectra of Dasy(o) (blue dotted line), Dasy(c) (blue solid line) and emission spectrum of Dasy(o) (red line).

The switching scheme of Dasy between the two photostationary states is schematically shown in Fig.5.3 (left). The red light is modulated while the UV light is switched on continuously. A_m stands for the amplitude of modulation and f_m stands for the frequency of modulation. It can be seen that the Dasy(o) fluorescence intensity can be controlled by red light that is much longer in wavelength than the absorption spectrum of the fluorescent species Dasy(o). The 365 nm UV light results in the intense emission of Dasy(o), at the same time inducing the isomerization from Dasy(o) to the non-fluorescent Dasy(c). The emission will be turned "off" when the sample is converted to 100% Dasy(c). If the sample is then exposed also to 660 nm red light that triggers isomerization from Dasy(c) to Dasy(o), the fluorescence will be turned "on" to establish the new photostationary state induced by UV and red light simultaneously. The rate constant of this process is referred to as k_{obs}. The emission of Dasy(o) can be switched "off" again when red light is turned off as the sample is isomerized to the non-fluorescent Dasy(c).

The amplitude modulation results of Dasy in aqueous solution at ca. 20 µM with modulation frequencies of 10 Hz (top), 105 Hz (middle), and 205 Hz (bottom) are shown in Fig. 5.3 (right). The driver signal of the laser diode at 660 nm is shown in black line and the fluorescence change of Dasy is shown in the red line. When the modulation frequency is faster than the sample reaching the new photostationary state ($f_m > k_{obs}$), there will be not enough time for the fluorescence of Dasy to be switched to the two extreme points, zero and maximum level. It means that the observed intensity change, referred to as the modulation amplitude A_m, will decrease with the increased modulation frequency f_m. It can be seen clearly in Fig.5.3 that compared to the A_m at 10 Hz, the amplitude dropped to 7.3% when modulation frequency

increased to 105 Hz. The amplitude further dropped to 4.7% when frequency becomes 205 Hz. Based on experimental data and established theory, it is noticed that the A_m changes dramatically in the lower frequency domain while there is no distinct change in A_m anymore when the frequency is higher than 200 Hz. It is very encouraging to see that the A_m can still be clearly detected by lock-in amplifier even when the frequency is higher than 200 Hz.

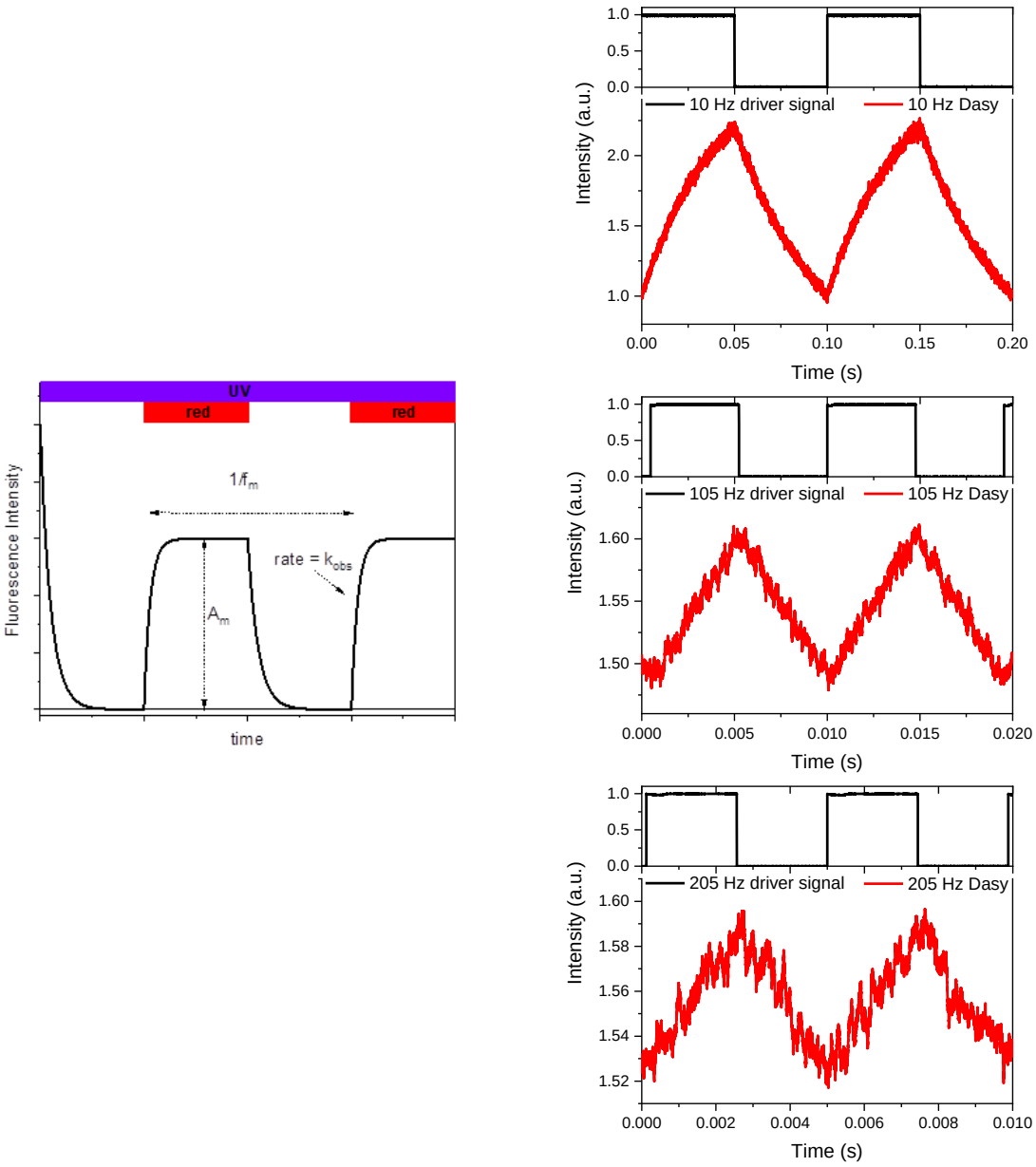

Figure 5.3. Left: Schematic description of Dasy switched between the two photostationary states. A_m is the modulation amplitude, f_m is the modulation frequency, k_{obs} is the observed rate constant for reaching the photostationary state induced by both UV and red light irradiation. Right: The amplitude modulation of Dasy in aqueous solution with modulation frequencies of 10 Hz (top), 105 Hz (middle), and 205 Hz (bottom). The 365 nm UV light is switched on continuously and the 660 nm laser diode is modulated at varying modulation frequencies (black lines). The modulated fluorescence of Dasy is shown in red lines.

To prove that the captured signal originates from the modulated fluorescence of Dasy(o), the following measurements were carried out: First, the steady state emission spectrum of a light source with maximum at 450 nm was recorded, which is shown in the blue line of Fig.5.4. After that, the emission spectrum was recorded when Dasy(o) was excited continuously at 365 nm and the detector was simultaneously irradiated with the 450 nm light source. It can be seen from the result shown in black line that the overall emission is dominated by the 450 nm light source (blue line) in this situation. For those measurements mentioned above, the lock-in detection was not applied and the red light at 660 nm was switched off. The next step was to start the modulation measurement. The modulated 660 nm red light was turned on with frequency at 10 Hz, and the detector signal was filtered by a lock-in amplifier set to the same frequency. As shown in Fig.5.4, the recorded emission spectrum shown in red line is in the same shape as Dasy(o) alone (see Fig.5.2) and the emission from the 450 nm light source is entirely suppressed. The result proved that through lock-in detection, the modulated signal from Dasy can be perfectly distinguished from an intense background emission by using amplitude modulated red light.

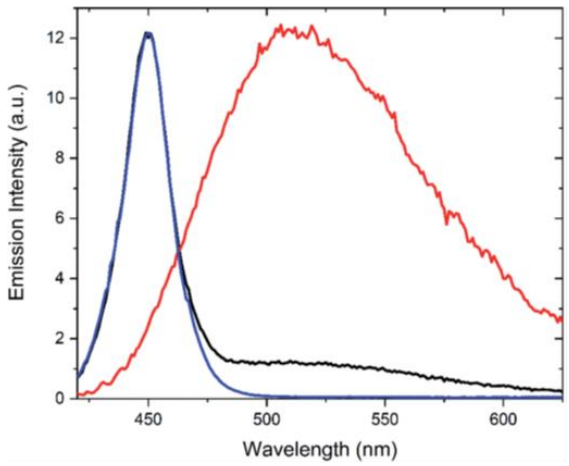

Figure 5.4. Normalized spectra of static emission from 450 nm light source (blue line), static emission from Dasy(o) + 450 nm light source (black line) and modulated emission (irradiation of continuous 365 nm and 10 Hz modulated 660 nm light) from Dasy(o) + 450 nm light source (red line).

To investigate if Dasy can display amplitude modulation also in cell imaging, a sample was prepared in medium solution containing L929 cells and Dasy(o) with concentration of 100 µM. It has been proved from results that the amplitude modulated fluorescence of Dasy is able to be detected within a biologically relevant environment. The detailed information about cell imaging measurements is shown in paper I.

In summary, here we introduced a fluorescent switch that has distinct fluorescence in the colorless open isomer in aqueous solution, which enables its emission modulation by red light, As the undesired background fluorescence or the scattered light is not affected by red light, the modulation signal of Dasy can be easily filtered out by lock-in detection. In addition, the modulation frequency of Dasy can be as high as 205 Hz with the signal sufficiently enough to be distinguished from the background. The outstanding properties and performance of Dasy, such as good water solubility, redshifted absorption spectrum, high fluorescence quantum yield, virtually 100% enrichment in both photostationary states, and rapid switching capabilities let it become promising to be applied in cell studies and microscopy experiments.

5.2 Single-color fluorescence photoswitching: turn-on mode fluorescent DAEs

The “turn-off” DAE photoswitches mentioned above is limited in some applications, such as super-resolution microscopy that requires an initial completely dark background.[42] On the other hand, the “turn-on” DAE derivatives in which the fluorescence can be increased dramatically when isomerizing to the closed form have been extensively studied and developed. A couple of illustrative examples are highlighted below. In 2009, Ahn and co-workers reported a DAE derivative where the fluorescence quantum yield of the closed isomer increased almost 100 times by oxidizing the sulfur atoms to sulfones. The fluorescence quantum yield can be further increased to 0.19 by introducing n-heptyl substituents at the reactive carbon. Additionally, by introducing the acetyl substituents at the 6- and 6′-positions of the benzothiophene-1,1-dioxide groups, the fluorescence quantum yield was improved up to 0.52.[107] Even so, the fluorescence quantum yields of those DAE derivatives are still lower than fluorophores that are commercially available, which is a challenge for their direct application in super-resolution imaging.[18]

To fulfill the requirements for super-resolution fluorescence imaging, a series of diarylethenes with sulfone derivatives was reported by Irie and co-workers in 2011. The fluorescence quantum yield of the closed isomer was further improved, which can be up to 0.88 by introducing both short alkyl substituents at the reactive carbon and aryl substituents to the benzothiophene-1,1-dioxide groups.[38] The isomerization from the open to the closed form is very effective whereas the quantum yield for the closed to open isomerization is very low, which meet excellently the requirements of super-resolution microscopy, such as photo-activated localization microscopy (PALM) and stochastic optical reconstruction microscopy (STORM).[42,77] To ensure the accuracy, enough photons need to be collected before the photoswitch isomerizes to the “off” state. With high fluorescence quantum yield and extremely slow switching “off” process, it is easy to collect sufficiently many photons before the photoswitch is isomerized back to the dark state. On the other hand, because of the efficient switching “on” process, the photoswitch can be easily populated with low intensity UV light. So far, the diarylethenes with sulfone derivatives have been successfully applied in different types of super-resolution microscopy, such as PALM and STORM and reversible saturable optical fluorescence transition (RESOLFT).[20,21]

One representative example of such application is reported by the Dominik group.[18] With the high fluorescence quantum yield, high photostability, a low quantum yield for the “on” to “off” switching, and reasonable quantum yield for “off” to “on” switching, the DAE derivative is a significant advantage for the super-resolved localization microscopy. By applying the photoswitch in super-resolved PALM, the resolution of the images increased ten times with respect to the diffraction limit. The structural details of copolymer cylindrical micelles are clearly visible in the super-resolved image compared to the conventional diffraction-limited image.

5.3 Multi-color switching of a molecular cocktail

Although single-color fluorescence "on-off" photoswitching has been used in many application fields, their application is still restricted because the molecule can only provide two different states: "on" and "off". In contrast, the multi-color fluorescence photoswitching systems can achieve multistate switching implying the existence of more than one emitting species contributing to the fluorescence and the associated spectral changes. Recently, such systems have been extensively studied and has opened the possibility in various applications, such as full-color reproduction,[24-28] data-security,[108-110] super-resolution fluorescence microscopy,[23,111,112] fluorescence labeling and bioimaging,[113,114] molecular logic and information storage[32,34,46]. The application potential of the multi-color fluorescence photoswitching systems has expanded far beyond single-color fluorescence photoswitching systems.[42]

Multi-color photoswitching systems can be further differentiated into two principally different ways: color-specific and color-correlated switching. Fig.5.5 illustrates the two different switching processes.[42] It can be seen from Fig.5.5 that for a color-specific process, the emission of one compound is switched between "on" and "off" by irradiation of light while the emission from another compound is not influenced during the process. In contrast, for color-correlated switching, emissions of both compounds are altered. The emission of one compound is turned "off", at the same time the emission of another one is turned "on" upon exposure to light.

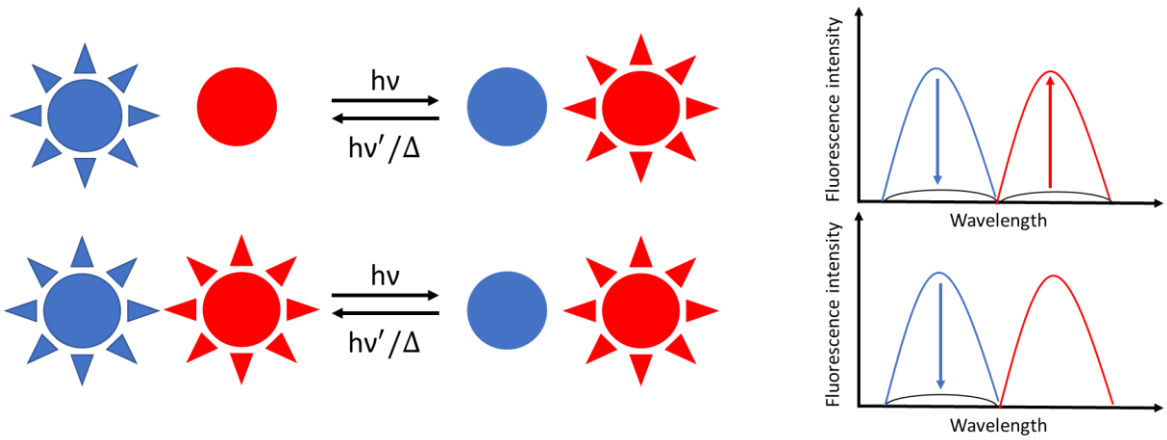

Figure 5.5. Schematic description of the color-correlated photoswitching system (upper case) and the color-specific photoswitching system (lower case).

Compared to the color-specific system, the color-correlated photoswitching allows for a much more distinct color change, as the increase in emission in one wavelength region is correlated with the disappearance of the emission in another wavelength region. The most common strategy for color-correlated systems is to combine a fluorophore that has higher energy emission with a "turn-on" photoswitch molecule that has lower energy emission.[42] By employing the ''static'' fluorescent dye as the energy donor and a molecular photoswitch as the corresponding acceptor, the FRET process is switched "on" and "off" during closing and opening isomerization process, thereby the fluorescence color is changed between the fluorophore and the photochromic fluorescent dye. The details of multi-color system based on FRET process will be explained in the next chapter. To trigger efficient FRET reactions, it is essential to keep the donor and the acceptor in close proximity. Therefore, various condensed systems such as nanoparticles,[115-118] organogels,[46,119] polymers[120-122] and covalently linked constructs[26,41,76,123-125] have been presented to ensure the efficiency of the FRET process. However, generally the flexibilities of those systems are restricted and complicated synthetic procedures are required for those approaches.

In our approach, a novel, extremely facile color-correlated photoswitching cocktail is designed by simply mixing two photochromic DAE derivatives in acetonitrile, which leads to a very flexible system as for choosing different fluorophores and adjusting their respective concentrations. The color changes of the cocktail are induced only by isomerization of the two monomer photoswitches without relying on any FRET reactions. The single light source at 381 nm is applied to trigger the color change and the virtually nondestructive emission readout is recorded by 410 nm excitation. Using light as the only external stimuli presents various advantages such as waste-free, non-invasive, and remote operation with the unsurpassed spatiotemporal control.

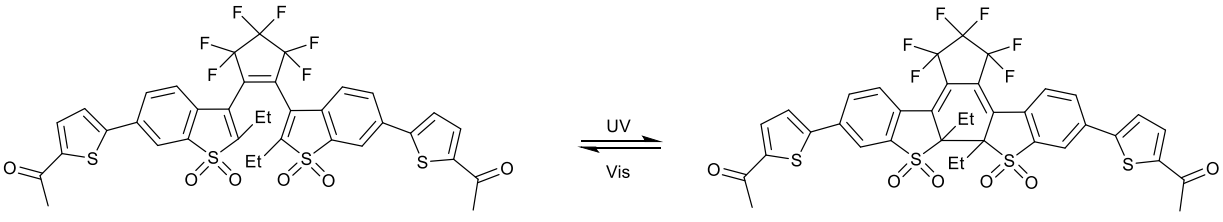

DAE9(o) DAE9(c)

Figure 5.6. The isomerization process of DAE9 between the open form and the closed form.

The structure and the isomerization scheme for the Dasy and DAE9 photoswitches are shown in Fig.5.1 and Fig.5.6 respectively. The relevant absorption and emission spectra are shown in Fig.5.7. It can be seen from Fig.5.7 that both Dasy(o) and DAE9(o) absorb almost exclusively in the UV region, which makes it easier to choose one wavelength of UV light to initialize the closing isomerization of both compounds. The opening reaction of both compounds can also be triggered by a common visible light source as both Dasy(c) and DAE9(c) absorb between 500 nm to 550 nm. There is no detectable emission from the closed isomeric form Dasy(c) or the open isomeric form DAE9(o). Dasy has its blue-green fluorescence only in the open isomeric form Dasy(o) with a quantum yield of 0.11 whereas DAE9 has orange fluorescence only in the closed form DAE9(c) with a quantum yield of 0.37 in acetonitrile.

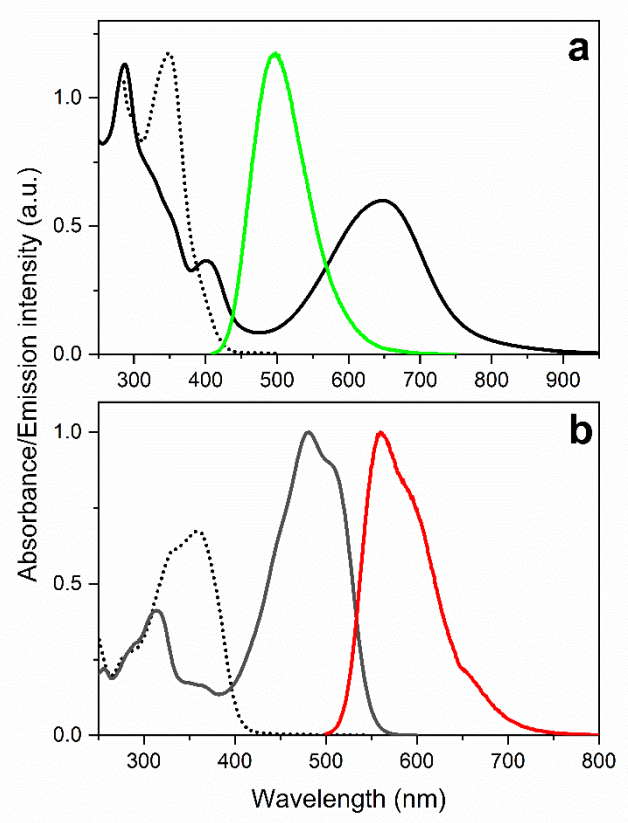

Figure 5.7. Absorption and emission spectra of Dasy (shown in a) and DAE9 (shown in b). The black dotted lines stand for the absorption spectra of the open isomers, the black solid lines stand for the absorption spectra of closed isomers. The green solid line stands for the emission of Dasy(o) and the red solid lines stand for the emission spectrum of DAE9(c).

The initial emission of the cocktail mixture of Dasy and DAE9 is blue-green fluorescence as both Dasy and DAE9 are in the open form and only Dasy(o) is fluorescent. By exposing the sample to 381 nm UV light, Dasy(o) and DAE9(o) are both isomerized to Dasy(c) and DAE9(c), respectively. Due to the UV induced isomerization, the blue-green emission of Dasy(o) will

gradually decrease while an increase of orange emission from DAE9(c) is expected. As the photostationary distribution of Dasy can be 100% shifted to the non-fluorescent Dasy(c) isomer, the system will show only orange emission of DAE9(c) in the end of the process as extended UV irradiation would lead to the disappearance of the blue-green emission from Dasy(o).

The isomerization quantum yields for the closing reactions are 0.52 and 0.13 for Dasy and DAE9, respectively, that is, 4 times difference between the isomerization quantum yields of Dasy and DAE9. As the isomerization rate of closing process is proportional to $\varepsilon_{open} \times \Phi_{iso}$ (open $\rightarrow$ close), the isomerization wavelength needs to be chosen accordingly to let rates of both isomerization processes become comparable, which is important for a continuous color change of the system. Here, 381 nm was selected as the excitation wavelength for the isomerization of the cocktail mixture since the ratio of $\varepsilon_{DAE9(o)}/\varepsilon_{Dasy(o)}$ is maximum at 381 nm. Based on the kinetics of closing isomerization process of DAE9(o) $\rightarrow$ DAE9(c) and Dasy(o) $\rightarrow$ Dasy(c) upon 381 nm irradiation, the isomerization time constants are 50.5 s and 105.2 s for Dasy and DAE9, respectively. Thus, the rates of the two closing isomerization reactions are comparable by using 381 nm as the excitation wavelength.

For the reading (excitation for emission readout) process, it is important that the excitation light does not induce any changes during the reading process to achieve a good "color stability" of the system. This implies that the excitation light for emission readout should be selected to cause minimal isomerization, at the same time maintaining a good signal to noise ratio of the emission spectra. As the emission quantum yields of both photoswitches are fairly high, excitation light 410 nm is selected for emission readout to grant the "color stability". It can be seen in Fig.5.7 that the absorption of the photochromically most active form, Dasy(o) is very low at 410 nm so that the isomerization from Dasy(o) to Dasy(c) is restricted during the reading procedure by 410 nm excitation.

It is also desirable for the cocktail mixture to have a constant overall emission intensity throughout the isomerization process. Therefore, the concentrations of two compounds in the cocktail mixture need to be alternatively adjusted to find the correct relations between Dasy(o) and DAE9(c). Fig.5.8 shows the overall emission changes of a cocktail containing ca. 35 µM Dasy and 2.3 µM DAE9 when exposed to 381 nm UV light. It can be seen clearly that the initial spectrum is dominated by emission of Dasy(o) while the final spectrum shows fluorescence mostly from DAE9(c). During the whole isomerization process, the intensities of overall emission are comparable for the cocktail mixture. It can be also seen by the CIE

coordinates in Fig.5.9 that the color of the cocktail system changes continuously from blue/green to orange, implying that the rates of Dasy and DAE9 isomerization reactions occur on a similar timescale.

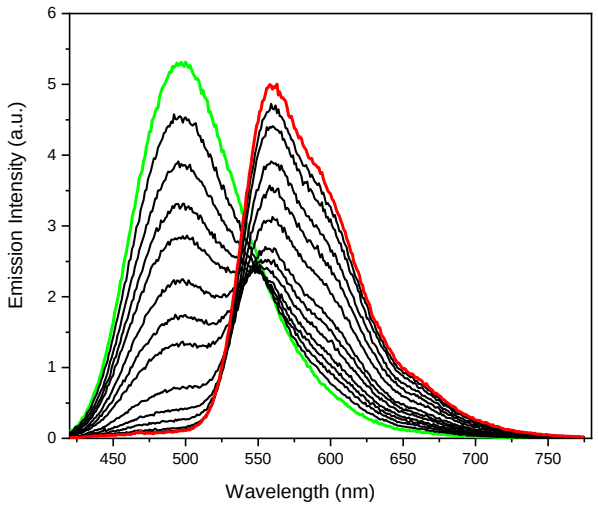

Figure 5.8. The emission changes of Dasy + DAE9 cocktail in acetonitrile by 381 nm irradiation for 0 s (green line), 5 s, 10 s, 15 s, 20 s, 30 s, 40 s, 50 s, 80 s, 110 s, 140 s, 200 s, 260 s, and 350 s (red line). The spectra were recorded upon 410 nm excitation.

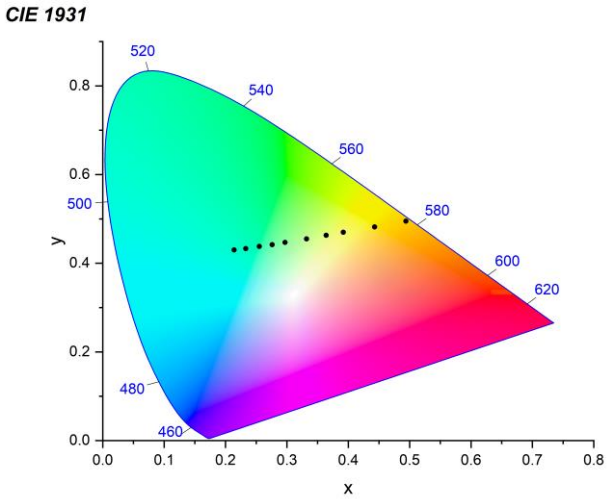

Figure 5.9. CIE coordinates of the emission changes of Dasy+DAE9 acetonitrile cocktail upon 381 nm irradiation. Irradiation conditions from left to right: no irradiation, 5s, 10s, 15s, 20s, 30s, 40s, 50s, 80s, and 350s by 381 nm UV light. All spectra recorded upon 410 nm excitation.

The stability of the system with respect to color changes over time was investigated by exposing the sample continuously to 410 nm excitation light. The outstanding color stability can be seen by the fact that there is no difference in the emission spectra after a time period equivalent to

recording 20 emission spectra and only minor changes observed after a time period equivalent to recording 50 spectra.

The operation of the cocktail system can be repeated with excellent reproducibility as there is no substantial photodecomposition of the sample after it is alternately exposed to 381 nm light and 523 nm light. Moreover, both the maximum and the minimum fluorescence intensities of two DAE derivatives remain at a fairly constant level throughout the cycling.

To verify that the observed color changes are only caused by isomerization rather than FRET reactions, TCSPC experiments were undertaken. The results show that there are no differences in the lifetimes of DAE9(c)/Dasy(o) monomers alone in acetonitrile compared to DAE9(c)/Dasy(o) in the cocktail mixtures, which indicates there is no quenching by FRET reactions in the cocktail system.

In summary, we presented a molecular cocktail in which the color of the system can be switched in a color-correlated fashion. The most appealing part of the system is that the dynamic color change only depends on the light-induced isomerization without requiring FRET or other excited state communication reactions. In addition, the cocktail system can be simply prepared by mixing two fluorescent DAE derivatives in bulk acetonitrile solution, which avoids the tedious synthesis or any design of complicated supramolecular systems. Moreover, the all- photonic operation let the system become non-invasive, waste free and able to be controlled remotely.

6. Intensity Modulation through FRET/PET Process

Although the fluorescence can be simply switched between "on" and "off" by the inherent changes in fluorescence quantum yield between the two isomeric forms, it is more common to combine a fluorophore with a photoswitch so that the system can be designed to have an efficient photochromic reactivity and a bright fluorescence simultaneously.[37] In this approach, generally the fluorescence is modulated either by Förster resonance energy transfer (FRET) or photoinduced electron transfer (PET).[42] To ensure the close proximity of the fluorophore and the photoswitch required for these reactions to occur, covalently linked systems have been widely used,[14,126-131] as well as other materials such as nanoparticles,[88,132,133] gels[134,135] and supramolecular assemblies.[136-138]

The working mechanism of such combined system is explained in Fig.6.1. In the beginning, the fluorescence from the fluorophore is "on" as the photoswitch is at the "quenching off" state (Q_{off}). Typically, with UV light irradiation, the photoswitch is isomerized to the "quenching on" state (Q_{on}) which initiates the FRET or PET process. The fluorescence of the system is thus switched "off". With visible light irradiation, the photoswitch is isomerized back to the "quenching off" state (Q_{off}) so that the fluorescence is again observed from the fluorophore. The fluorescence of the system can be switched "on" and "off" repeatedly by the reversible isomerization of the photoswitch.

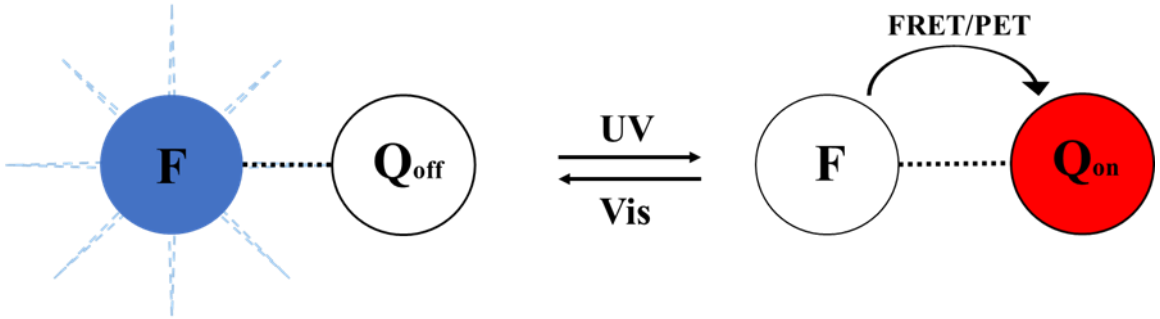

Figure 6.1. Schematic representation of intensity modulation by FRET/PET process.

In DAE derivative-based FRET systems, the fluorescent dye acts as an energy donor and the photochromic molecule is the corresponding acceptor. One prerequisite for an efficient FRET reaction is to have a sufficiently large spectral overlap between the emission spectrum of the donor and the absorption spectrum of one photochromic isomer. In contrast, the overlap

between the emission of donor and the absorption of the other isomer should be negligible. It is thus desirable for DAE photochromic molecules to exhibit a large spectral shift in absorption during isomerization as Fig.6.2 illustrates.

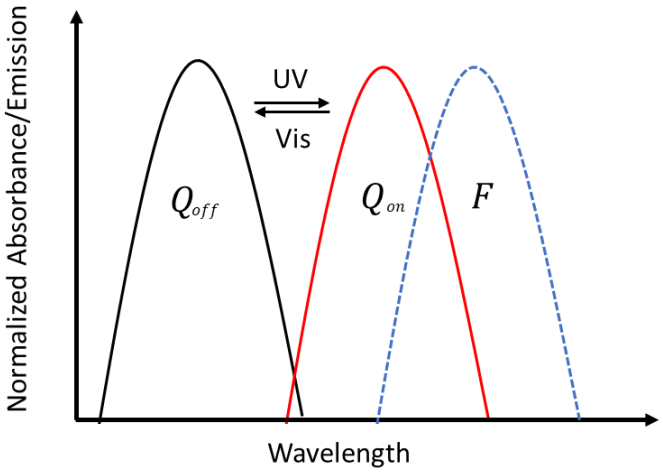

Figure 6.2. Schematic example of donor emission spectrum and acceptor absorption spectra for FRET process. The absorbance of quenching "off" state (Q_{off}) is shown as black solid line and the absorbance of quenching "on" state (Q_{on}) is shown as the red solid line. The fluorescence of donor is shown as the blue dashed line. Because of large spectral overlap between the donor fluorescence and the absorbance of Q_{on}, FRET is initiated when the photoswitch isomerized to Q_{on} state by UV light. As there is no spectral overlap between the absorbance of Q_{off} state and the donor fluorescence, no FRET reaction occurs when the photoswitch is isomerized to Q_{off} state by visible light.

In the FRET process, the fluorophore is non-radiatively deactivated by sensitizing the excitation of the photochromic acceptor. Thus, to initiate the FRET, two excitation processes are required: one process is to excite the photochromic molecule to trigger the isomerization to the "Acceptor-on" form that has a large spectral overlap with donor emission; another one is to excite the fluorophore for emission readout.

One early example of a DAE-based FRET system is shown in Fig.6.3.[139] The dyad is designed with a DAE photochromic acceptor and an anthracene donor fluorophore. The fluorescence of the anthracene unit has only substantial overlap with the absorption spectrum of the closed isomer of the DAE molecule. Therefore, upon UV induced isomerization from the DAE open form to the closed form, the energy transfer process will be triggered from the anthracene donor fluorophore to the DAE molecule that is now in the "quenching on" state, which leads to the fluorescence of the system being turned "off" (fluorescence quantum yield lower than 0.001). In contrast, once the DAE photoswitch is isomerized back to the open "quenching off" state by visible light, there is no FRET reaction and the fluorescence of the anthracene fluorophore is turned "on" again with the fluorescence quantum yield of 0.73. In this way, the fluorescence

of the system can be turned “on” and “off” reversibly by switching the FRET process through UV and visible light.

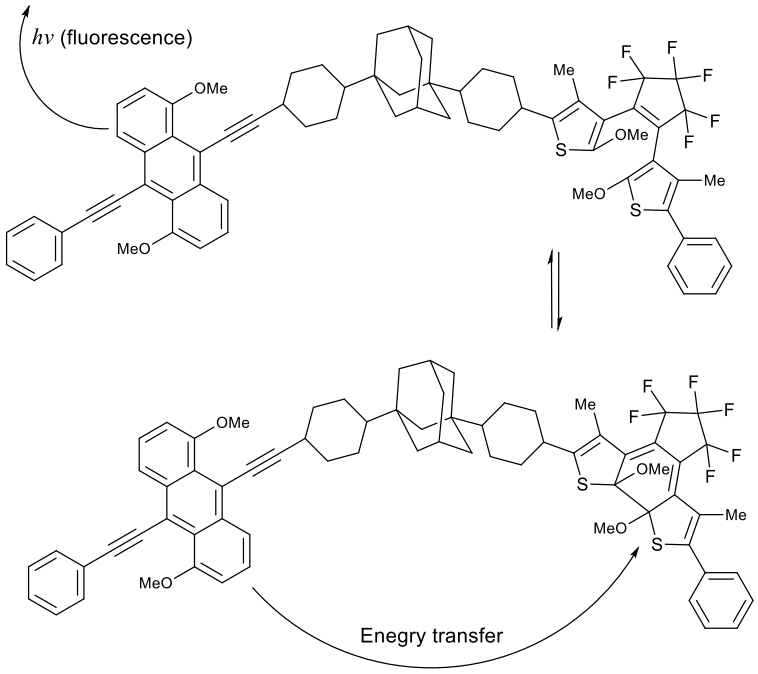

Figure 6.3. Interconversion of a dyad consisting of a photochromic DAE acceptor and an anthracene fluorophore donor. The upper structure displays fluorescence from the anthracene unit when the DAE photoswitch is in the open “quenching off” state. In the lower structure, the fluorescence is quenched by energy transfer (FRET) when the DAE photoswitch is isomerized to the closed “quenching on” state.

It can be seen from equation (2.10) that the rate of FRET quenching is enhanced by the increased spectral overlap between the emission of the donor fluorophore and the absorbance of the photochromic acceptor molecule as the rate constant of FRET, $k_T(r)$, is proportional to the spectral overlap integral, $J(\lambda)$. In addition, the efficiency of the FRET process is highly sensitive to the distance between the donor and the acceptor, as $k_T(r)$ is proportional to $1/r^6$, where r is the donor-acceptor distance. This implies that a small change in distance between the donor and the acceptor can result in a significant difference in the FRET rate. Typically, the distance between the donor and the acceptor needs to be within 10 nm for the occurrence of FRET processes.

Except for the FRET process, fluorescence switching can also be achieved based on the PET mechanism in which an electron is transferred between the fluorophore and the photochromic molecule. The electron transfer process can be activated or deactivated by sufficiently large differences in the redox potentials between the two isomers. Compared to FRET, the PET

process can be much more influenced by the distance between electron donor and acceptor. It is because FRET arises from a dipole-dipole interaction, yielding the $1/r^6$ distance dependence.[51] In contrast, the PET process requires orbital overlap between the donor and the acceptor, which decreases exponentially with distance.

The driving force for PET is calculated from equation (6.1). In the equation, E_{Ox} stands for the oxidation potential of the donor, E_{Red} stands for the reduction potential of the acceptor, e stands for the elementary charge, ΔE_{00} stands for the energy change associated with the S_0 to S_1 transition, ε_0 is the vacuum permittivity, ε_r is the dielectric constant of the medium, d is the distance between the electron donor and the acceptor. For photochromic molecules, the reduction or oxidation potential of the molecule can be changed substantially through the isomerization process, which can switch "on" and "off" of the electron transfer process between the fluorophore and the photochromic molecule.

$$\Delta G^0 = e[E_{Ox} - E_{Red}] - \Delta E_{00} - \frac{e^2}{4\pi\varepsilon_0\varepsilon_r d} \qquad (6.1)$$

One example is a molecular dyad containing a perylene bisimide that is covalently linked to a diarylethene photoswitch.[140] The system has the fluorescence around 750 nm whereas the emission is switched "off" when the system is exposed to UV light that triggers the isomerization of the diarylethene photoswitch from open to the closed form. Through calculation, it is noticed that the ΔG^0 of PET process is 0.37 eV for the dyad with the open form ($Open^-$ - Dye^+) and −0.03 eV for the dyad with the closed form ($closed^-$ - Dye^+). It means the PET process is only thermodynamically favorable between the fluorophore and the closed isomer. Therefore, the PET process is switched "off" initially when the diarylethene photoswitch is in the open form and switched "on" simultaneously when the photoswitch is isomerized to the closed form.

As the work conducted in this thesis focuses on DAE-based FRET systems, the PET process will not be further elaborated on here.

6.1 Emission color tuning by FRET process

It can be noticed that for the mechanism mentioned above, the FRET process occurs without the appearance of a photon (given that the FRET acceptor is non-fluorescent), which implies that the overall fluorescence of the system switched "off" in the quenching state. The downside of such system is that the photon is wasted in the end and there are only two states with respect to the fluorescence properties: "on" and "off". This imposes restrictions in practical applications. It would be more beneficial if multi-color photoswitching can be constructed by the donor-acceptor pairs, that is, if the FRET process does not necessarily imply the loss of the photon.

To surmount the limitations of single-color fluorescence photoswitching, the FRET-based systems of fluorophore-photoswitch pairs have been intensively studied and have shown great promise in displaying stimuli-responsive emission color.[141-149] The mechanism of one system is shown in Fig.6.4. Compared to the single-color photoswitching system, one additional prerequisite of multi-color photoswitching systems is that the photochromic acceptor has to be fluorescent in its FRET-active form.

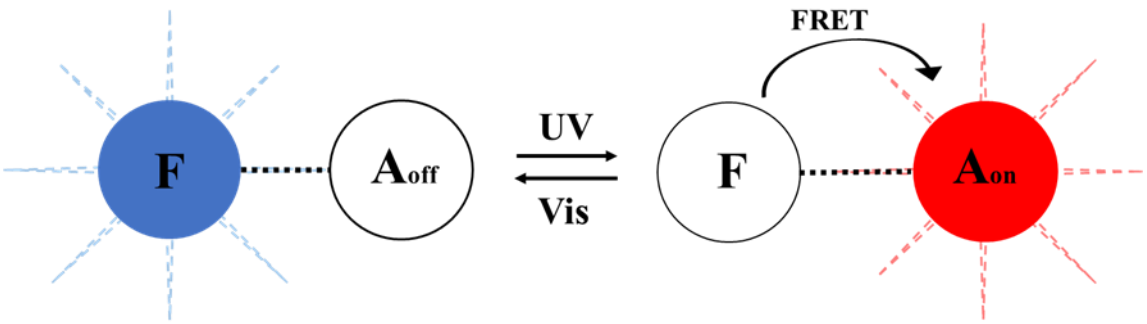

Figure 6.4. Schematic explanation of emission color tuning of the fluorophore-photoswitch pair by FRET process.

At the beginning of the process, the fluorescence of the system is emitted from the fluorophore when the photoswitch is at the acceptor "off" form (A_{off}). When the system is exposed to UV irradiation, the photoswitch is transformed to the acceptor "on" form (A_{on}), which initiates the FRET process. As the A_{on} form is fluorescent, the emission of the acceptor starts to appear while the emission of the fluorophore begins to be quenched. Therefore, the emission color is a mixture of the donor and the acceptor in intermediate states (when both isomeric forms of the dyad are present) and the color of the system is changed gradually from donor-centered to acceptor-centered as the photoisomerization process is proceeding. This means that any

emission color between the donor and the acceptor can be achieved during the isomerization process. When the isomerization process is finished, the donor will be largely quenched and the emission color is dominated by the acceptor.

There are some key points that need to be addressed in the design of such multi-color system. Firstly, to maintain an overall high emission intensity throughout the isomerization process, the fluorescence quantum yield of the photochromic acceptor should be comparable to that of the fluorescent donor fluorophore, i.e., on the high end. In addition, to achieve a distinct change in the emission color, it is vital that the photoswitch can be fully transformed from A_{off} to the A_{on} state so that the majority of the donor fluorophores are FRET-quenched.

Our group has previously demonstrated how the perceived emission color can be changed continuously from the fluorophore donor emission to emission of the photochromic acceptor.[115] The donor of the system was chosen to be 9, 10-diphenylanthracene (DPA) that has emission centered between 400 nm and 450 nm. The sulfone derivative of a diarylethene (DAE) photoswitch was used as the acceptor whose open form has no absorption above 400 nm while the closed form has the maximum absorbance around 450 nm. The DAE acceptor has the advantage of emitting intense fluorescence in the closed form (emission quantum yield 0.75 in acetonitrile), which ensured the overall high and comparable emission intensities of different emitting states. Moreover, the sample can be enriched to 100% of the respective isomeric form by both the UV and the visible light-induced reactions (closing isomerization quantum yield = 0.42, opening isomerization quantum yield = 4.0×10^{-4}). It means the DAE can be fully transformed to the acceptor "on" form and the process can be reversed by exposure to visible light.

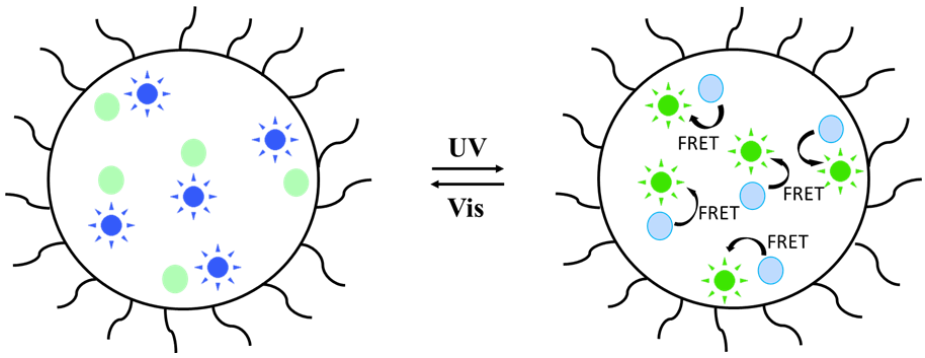

Figure 6.5. Schematic illustration of a polymer micelle containing donor DPA (blue dots) and acceptor DAE (green dots). Photoswitching of DAE from open to closed form allows for FRET, resulting in tuning of the system emission color.

In this system, the donor and the acceptor are encapsulated in polymer micelles to ensure the close proximity required for an efficient FRET process. The design of the system is shown in Fig.6.5. The blue fluorescence of the DPA donor fluorophore is initially the only emission present. However, the emission of the donor is FRET-quenched by the UV induced isomerization of the acceptor to the colored FRET-active form. At the same time, the green emission of the acceptor starts to appear. In the end, the system color is dominated by the green emission from the acceptor.

The changes in the overall emission spectrum are shown in Fig.6.6 (left).[115] The initial emission spectrum is shown in the black line. It can be noticed clearly that at the beginning there is only emission from DPA. Through UV irradiation, the intensity of the DPA emission keeps decreasing, at the same time the emission intensity of the DAE closed form (DAEc) keeps increasing. In the end, the emission from DPA donor is largely quenched and the fluorescence of the system mainly stems from DAEc. It can be also seen from the Commission of Internationale d'Eclairage (CIE) diagram in Fig.6.6 (right) that the observed emission color changes along the straight line from DPA blue emission to the yellow-green emission of DAEc.[115] The intermediate colors along the line were all observed during the isomerization process. The process was reversed by visible light exposure, triggering the ring-opening isomerization process.

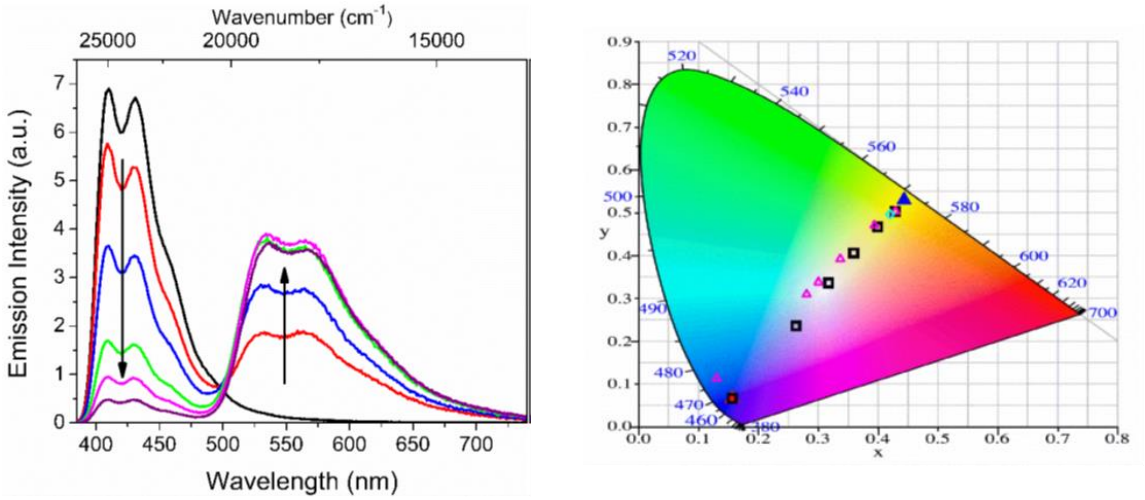

Figure 6.6. Left: Overall emission spectra of polymer micelles containing DPA and DAE. The initial spectrum (black line) was excited at 415 nm to avoid any isomerization induced by the excitation light. The corresponding emission changes are shown by arrows upon gradual exposure to 365 nm UV light.[115] Right: CIE coordinates showing the color changes of micellar cocktail containing DPA and DAE upon UV exposure (black hollow squares) and visible light exposure (magenta hollow triangles) as well as coordinates for DPA alone (red solid triangle) and DAEc alone (blue solid triangle).[115]

6.2 Multi-color tunable RGB molecular system

Although several multi-color photoswitching systems have been designed and developed, in most of the reported studies the variation of the achieved emission colors is limited.[30,41,43,46,108,115,122,142,150-152] Especially, achieving a full color display with a red–green–blue (RGB) switching system remains as a major challenge.[153-155] In principle, wide-spectrum and even full color emission can be produced by making use of fluorescence of three original color red (R), green (G), and blue (B).[37,156] Therefore, the system becomes more complicated as it needs to achieve all color in RGB area by controlling fluorescent photoswitching in the multicomponent system.

To date, several strategies have been proposed to achieve a broader range of emission color in RGB full color systems. One common way is the additive mixing, that is, to blend the three original colors in different mixing ratios.[155,157-159] The downside of this approach is either that the emission output is "static"- the color is not able to be changed in one system, or that the tunable colors that can be achieved from the system are very limited.

For example, Akagi and co-workers demonstrated RGB photoswitching systems by mixing photoresponsive and non-photoresponsive fluorescent nanospheres.[159] To achieve RGB, three different systems are prepared and each system contains red, green and blue nanospheres, two of which consist of DAE molecules at the side chains while the other one does not have any DAE moieties. In each system, three nanospheres are mixed at the appropriate ratio to generate white light emission at the initial state. When the system is exposed to UV light, the DAE molecule is transformed to the closed isomer and the energy transfer is initiated from the backbone of the polymer to the closed isomer of the DAE molecule. Thus, the colors of two nanospheres that contain DAE moiety are quenched while the color remains for the nanosphere without DAE molecules. In this way, three different systems can achieve color changes from white-to-blue, white-to-green and white-to-red respectively. The system looks attractive as a tunable fluorescent system. However, the variation of the system is very limited as the color can only change between white and red/blue/green. In addition, three individual nanosphere mixtures need to be created to generate the RGB system, which leads to the preparation work becoming more complicated.

Although some other fluorescent systems have been designed to be color-tunable, either the procedure is complicated in that various treatments require physical access/contact, or the

system has to be altered for any change of emission color.[25,154,160-169] The major downside with all systems mentioned above is that it is not possible to tune the emission color in a closed system as the external stimulus is required to be in close contact, which results in the exclusion of remote operation.

As for our approach, reported in paper III, it is the first time that photochromic molecules are successfully applied for RGB full color reproduction where the emission color can be continuously changed from blue to green or blue to red or any linear combinations in between, only by photonic stimuli.[24] Using light instead as the external stimulus eliminates the need for physical access. Moreover, it is appealing that the all-photonic system allows for full-color reproduction, that is, all colors in the visible spectrum can be generated from one and the same sample. The function of the system can be realized by orthogonally controlled FRET processes between a perylene donor and two diarylethene photoswitches that have green and red emission color in the closed form, respectively. The color of the system is switched from blue to green or blue to red through a color-correlated fashion by selective isomerization of the two photoswitches. In addition, all emission colors within the red-green-blue (RGB) system can be achieved by isomerization of both photoswitches.

In this designed molecular system, the donor perylene and the two photochromic acceptors are encapsulated in polymer micelles in aqueous solution. There are several advantages of using polymer micelles for encapsulation. Firstly, it is easy to adjust the concentration of any individual component (that is, the relative concentrations of the chromophores) without requirement of tedious synthesis. Secondly, components inside the micelle are enforced being in close proximity with each other, which ensures the distance between donor and acceptor is close enough for efficient FRET to occur. Thirdly, it is very easy to vary the nature of the components used, simply by changing the ingredients in the cocktail. This is a much more flexible approach than having to synthesize covalently linked triads whenever you want to replace any of the chromophores in the system. The structure of the amphiphilic copolymer forming the micelles is shown in Fig.6.7 (left). The hydrophobic domains associate with the hydrophobic core and the hydrophilic domains enable water solubility. Therefore, the amphiphilic polymers can self-assemble into micellar nanoparticles spontaneously. The ST-7-8 copolymer was designed and synthesized by collaborators at University of Miami. A photograph showing the emission from the three fluorophores (perylene, DAEg(c) and DAEr(c)) alone in the micelles is shown in Fig.6.7 (right).

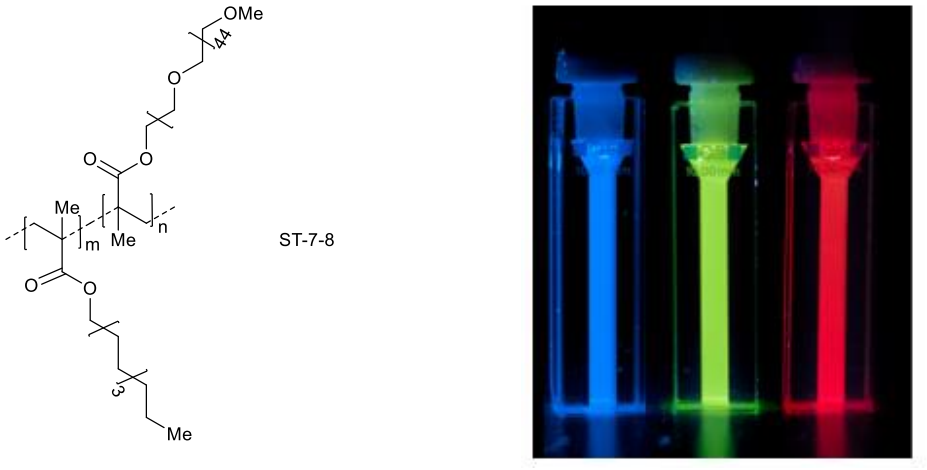

Figure 6.7. Left: structure of the ST-7-8 copolymer. m:n = 4:1. Right: the photo of fluorophores alone (left to red: perylene, DAEg(c) and DAEr(c)) in the micelles upon 365 nm excitation.

The structures and the isomerization scheme for perylene (per) and the two photochromic DAE derivatives, DAEg and DAEr (the g and the r stand for the emission color of the closed isomers, green and red, respectively) are shown in Fig.6.8. It can be noticed that there is no significant emission from the open form of the DAE derivatives, DAEg(o) and DAEr(o), while the closed isomers DAEg(c) and DAEr(c) have green and red emission respectively. In addition, the FRET process can happen between the donor perylene and DAEg(c) or DAEr(c), due to the pronounced spectral overlap between the absorption spectra of these forms and the perylene emission spectrum.

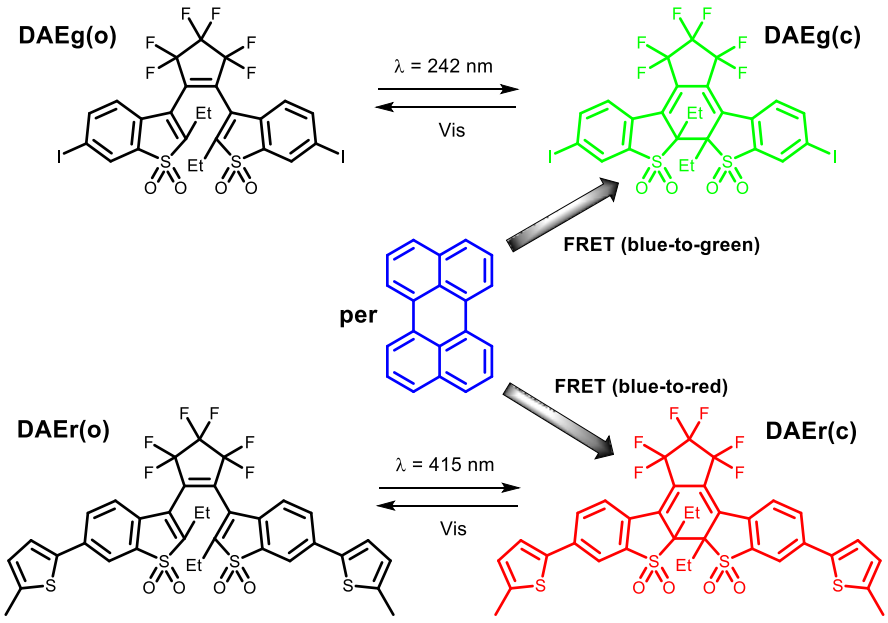

Figure 6.8. Structures of perylene, DAEg and DAEr and photo induced isomerizations as well as FRET processes (shaded arrows) with accompanying changes in the emission color.

Compared to the large spectral overlap between perylene emission and the absorbance of DAEg(c) and DAEr(c), there is almost no spectra overlap between the perylene emission and the absorbance of DAEg(o) and DAEr(o). It implies that the FRET can only happen between perylene and the closed form of DAEg and DAEr. During the FRET process, not only the blue emission of donor is quenched, but also the fluorescence of the DAE acceptor is sensitized, which implies that the color of the system can be dynamically tuned from donor emission blue to green emission or red emission of acceptor depending on the selective closing isomerization of DAEg or DAEr.

In principle, to achieve color changes from blue to green or blue to red, the energy transfer needs to be selectively activated from the donor fluorophore to one of the photochromic acceptors, that is, the other photochromic molecule should not be influenced during the isomerization process. Otherwise, instead of achieving pure green or red, a color mixture will be reached. Therefore, it is very important to realize the selective isomerization of DAEg (o) → DAEg(c) and DAEr(o) → DAEr(c) so that only one of the photochromic acceptors is involved in the FRET induced color change. To control the isomerization process, it is critical to choose the isomerization wavelength for the corresponding photochromic isomerization. For the process of DAEr(o) → DAEr(c), the 415 nm is selected as there is no or very little absorbance from DAEg(o) at this wavelength. As for isomerization of DAEg (o) → DAEg(c), 242 nm UV light is chosen because the molar absorption coefficient of DAEg(o) is the largest compared to DAEr(o) at this wavelength. Although the 242 nm is also absorbed by DAEr(o), the isomerization quantum yield for the DAEg(o) → DAEg(c) reaction is substantially higher than for DAEr(o) → DAEr(c) (0.50 vs. 0.0005 in acetonitrile), implying that the 242 nm exposure is expected to be virtually specific for DAEg(o) → DAEg(c).

For the readout process (excitation for emission readout), the excitation wavelength 423 nm was chosen to minimize the occurrence of any isomerization process so that the color of the system can stay stable during the readout process. In addition, perylene absorbs strongly at 423 nm while this wavelength is short enough to allow for recording virtually the whole emission spectrum without interference from the excitation light.

After the isomerization wavelengths and the excitation wavelength were chosen, another challenge for the project was to adjust the concentration of each component in the tri-component cocktail as the emission intensities of the initial state and final states of the system

should be comparable. Moreover, the concentrations of DAEg and DAEr cannot be too high, as this will imply D-A distances in the micelles that eventually will lead to a very efficient, and undesired, PET quenching of the perylene excited state. The concentrations of DAEg and DAEr cannot be too low either, as this will lead to inefficient FRET reactions and much smaller overall changes in the emission color. For FRET to occur efficiently, the distance between the donor and the acceptor should be shorter than the critical Förster radius R_0. As for the perylene concentration, it was chosen to allow for only one perylene molecule in each micelle to eliminate undesired redshifted emission from exciplexes.

In addition, there is another factor that influences the adjustment of concentrations in the tri-component system, that is the emission of DAEg(c) can be FRET-quenched by DAEr(c), which leads to the increase of red emission at the expense of green emission. This means that during the isomerization of DAEg(o) → DAEg(c), once more DAEr(c) are formed, the achieved color of the system will be inevitably become more yellow instead of green. In contrast, if the concentration of DAEg(c) is excessively high during the isomerization of DAEr(o) → DAEr(c), the red emission result will be obscured by that of DAEg(c) as 415 nm light is not selective for DAEr(o) → DAEr(c) isomerization to 100%. Thus, there are several trade-offs to be considered to balance the concentrations of DAEg and DAEr.

The optimal bulk concentrations of the tri-component cocktail were found to be [perylene] = 0.45 μM, [DAEg] = 3.7 μM, [DAEr] = 1.1 μM, and [micelles] = 0.31 μM through measurements. The schematic depiction of tri-component polymer micelle with the chosen concentrations is shown in Fig.6.9. In each micelle, 1 perylene, 12 DAEg, and 4 DAEr molecules are encapsulated.

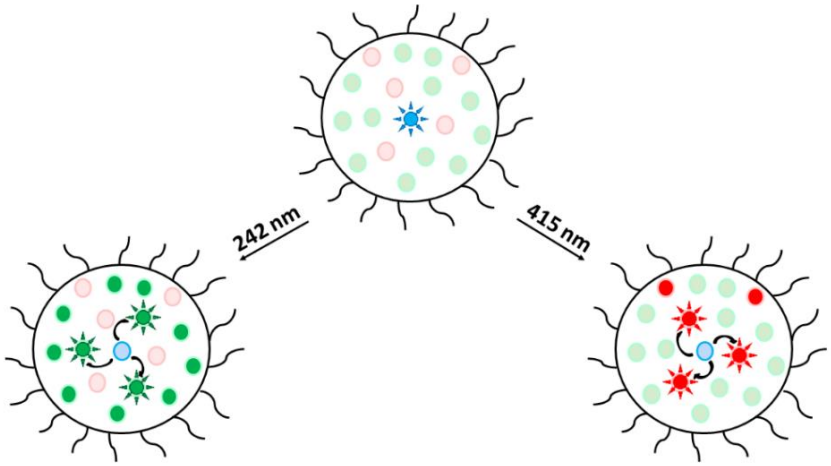

Figure 6.9. Schematic description of tri-component polymer micelle cocktail consisting of perylene (blue dot), DAEg (green dots) and dear (red dots).

For the chosen concentrations of the tri-component cocktail, based on a perylene fluorescence quantum yield of 0.85 in the polymer micelles and assuming κ^2 = 2/3 (freely rotating chromophores), R_0 values were calculated to be 45 Å and 51 Å for the perylene - DAEg(c) and perylene -DAEr(c) FRET-pairs, respectively. The donor-acceptor distances in the micelles (average nearest donor-acceptor distance) is calculated to be $R_{D\text{-}A}$(perylene-DAEg) = 28 Å and $R_{D\text{-}A}$(perylene -DAEr) = 38 Å. This implies expected FRET efficiencies of 95% for perylene-DAEg(c) and 84% for perylene-DAEr(c). This is comparable to the experimentally obtained values of around 90% FRET efficiencies for both situations.

To prove that FRET is the dominating quenching mechanism for color changes of the system with the chosen concentrations, excitation spectra of the bi-component cocktails perylene-DAEg(c) and perylene-DAEr(c) were recorded with the emission wavelength in regions where perylene does not emit. After comparison, it is found that the shapes of the excitation spectra are very similar to the absorption spectra of the bi-component cocktails, which strongly suggests highly efficient FRET between the perylene and DAEg(c)/DAEr(c). This is further strengthened by the results from TCSPC experiments. The fluorescence lifetime of perylene alone in the micelles is 4.8 ns while this number is decreased to 0.90 ns and 0.51 ns in the tri-component cocktails containing mainly perylene-DAEg(c)-DAEr(o) and perylene-DAEg(o)-DAEr(c), respectively. All those data proved that the chosen concentration combination of the tri-component system ensured the efficient FRET process that induces the color change from the donor to the respective acceptor.

After the concentration of each component in the system was determined, another factor needs to be considered: the applied isomerization times. For isomerization of DAEg, most of DAEg(o) can be isomerized using rather short illumination time due to the fairly high isomerization quantum yield. If the illumination time is too long, more DAEr(o) will start to be isomerized to DAEr(c), which will lead to the appearance of undesired red fluorescence. Therefore, it is necessary to carefully balance the 242 nm UV irradiation time. The time of 415 nm irradiation however is not that critical, as although a small part of DAEg(c) can be formed during irradiation, it is possible for the majority of DAEg(c) to be quenched by DAEr(c). All these considerations taken into account, the times were set to 600 s of 242 nm irradiation, and 2.5 h of 415 nm irradiation. Please note that the rather extensive irradiation times are explained by the fact that the isomerization light was the light from the spectrofluorometer xenon lamp after passing through the monochromator, resulting in moderate light intensities.

After all the measurement conditions were decided, the emission spectra from the tri-component cocktail were recorded as shown in Fig.6.10 (a). As a comparison, Fig.6.10 (b) shows the normalized emission spectra of perylene alone, DAEg(c) alone, and DAEr(c) alone in the polymer micelles. The fluorescence quantum yields of the system were determined to be 0.85 for perylene, 0.23 for DAEg(c), and 0.43 for DAEr(c).

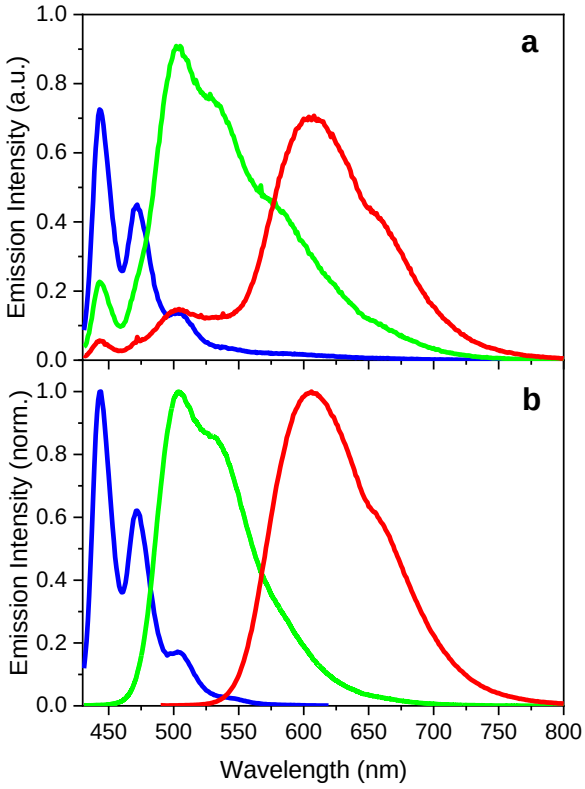

Figure 6.10. (a): Emission spectra of the tri-component micelle cocktail before UV irradiation (blue line), after exposure to 242 nm light (green line) and after exposure to 415 nm light (red line). (b): Normalized emission spectra of perylene (blue line), DAEg(c) (green line), and DAEr(c) (red line) alone in the polymer micelles.

For the initial state, it can be seen from Fig.6.10 (a) that the spectrum is virtually identical to that for perylene alone in Fig.6.10 (b), apart from a weak tail at the red end of the spectrum. This tail is ascribed to small amounts of the closed, fluorescent isomers of the DAE units present already at the beginning of the experiment. Compared to the emission intensity of perylene alone in the polymer micelle, the intensity of perylene in the tri-component system dropped by ca. 70% in the cocktail, tentatively ascribed to quenching by electron transfer reactions. After irradiation at 242 nm, it can be seen from the spectrum that the emission is dominated by DAEg(c) as expected. The spectral shape of the green emission in Fig.6.10 (a) is very similar to that in Fig.6.10 (b). Except for a small part of unquenched perylene, there are

minor emission features from DAEr(c) in the green spectrum of the tri-component system, as 242 nm light is not 100% selective for DAEg(o) isomerization. After irradiation at 415 nm, there are minor spectral features from perylene and DAEg(c) at shorter wavelengths compared to the red emission of DAEr(c) alone in the polymer micelle. However, it is clear that the emission of the system is mostly contributed by DAEr(c).

It is also encouraging to notice in Fig.6.11 that the CIE coordinates of the three emission spectra from the cocktail are very close to those of the pure monomer samples. For all emission results shown above, spectra are recorded using one and the same excitation wavelength which implies that the observed color change is not due to any influence of the excitation during the readout process.

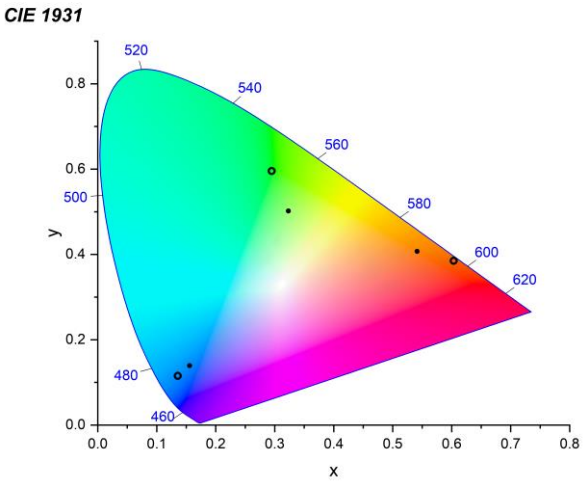

Figure 6.11. CIE coordinates for the emission from the fluorophores alone in the micelles (hollow circles): perylene (0.14, 0.12), DAEg(c) (0.29, 0.60), and DAEr(c) (0.60, 0.38) as well as emission of the tri-component micelle cocktail (solid circles) before UV irradiation (0.16, 0.14), after exposure to 242 nm light (0.32, 0.50) and after exposure to 415 nm light (0.54, 0.41).

The next step is to see if all colors within the RGB triangle can be generated by isomerization of both DAE derivatives. The tri-component system was therefore exposed to a large number of combinations of 242 and 415 nm exposures, and the corresponding CIE coordinates are shown in Fig.6.12. It is exciting to see that all colors within the RGB triangle can indeed be reproduced.

The final step is to investigate the color stability and the thermal stability of the tri-component cocktail. A selected intermediate state of the system was exposed to 423 nm light for 65 min that is equivalent to the collection of 100 emission spectra at this excitation wavelength. No significant differences are seen from the spectrum, which implies the color stability of the

system is sufficiently good. The thermal stabilities of the DAEg(c) and DAEr(c) in micelle were also been tested and there is no significant spectral change observed in the dark after 20 h.

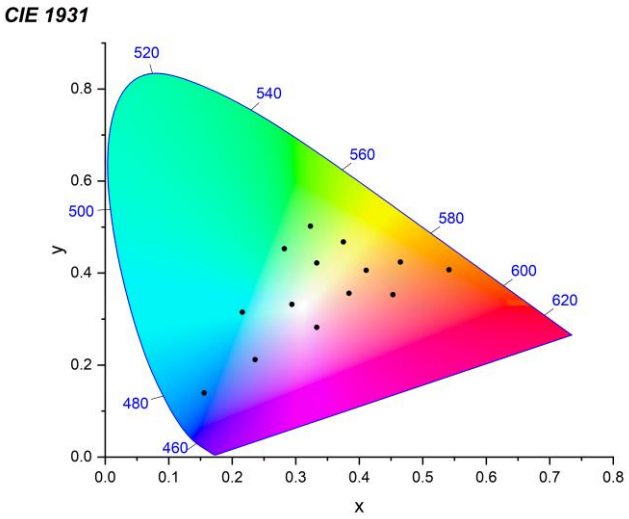

Figure 6.12. CIE diagram showing emission colors generated by RGB tri-component molecular system.

In summary, here we designed an all-photonic full color RGB system based on molecular photoswitches. The process relies on the orthogonally controlled FRET processes that are initialized by selective isomerization of the relevant photoswitch acceptor and the color of the system can be tuned dynamically within the RGB region. The light is used as the only external stimulus that eliminates the need for any physical access, which enables the system to be waste-free, non-invasive and delivered with extremely high spatiotemporal precision.

6.3 Molecular logic

It is easily realized that the "on-off" response in fluorescence intensities that follows isomerization of fluorescent photochromic systems can be useful in situations where binary (and higher order) responses are key to function. Binary logic and Boolean algebra qualify as such. When molecules are used for the generation of the binary output signals, it is referred to as molecular logic. Photochromic molecules are very well suited for this purpose, as the state of the system can be conveniently controlled by light inputs. Below, our attempt toward a photochromic FRET-based fluorescent logic system will be described. But first: the basics.

Conceptually, the computer programming languages used today is a primary modern application of Boolean algebra. Boolean algebra is also known as binary algebra. It was introduced by George Boole in his first book The Mathematical Analysis of Logic in 1847.[170] The operation of Boolean functions are represented as binary numbers: 1 = true and 0 = false. Such binary digit is also called a bit, which is the basic unit of information for computational logic. Compared to the elementary algebra that deals with numerical operations, Boolean algebra uses logic operations. The core Boolean functions are conjunction (AND), disjunction (OR) and negation (NOT), as opposed to addition, subtraction, multiplication, and division.

In 1993, de Silva and co-workers reported the first molecular photoionic AND gate where the fluorescence emission intensity could be chemically controlled by the addition of protons and Na^+ ions as inputs.[171] The input/output characteristics can be performed by the use of a fluorescent molecule equipped with receptors for the respective input. The research attracted a massive amount of interest over the past few decades and lots of researchers are trying to design different molecule-based systems that can replicate the Boolean logic gates or even more complicated logic devices.[29,69,172-188]

Among different molecular logic devices, photochromic molecules stand out as promising candidates in logic operation.[30,32,34,182,187,189-191] With the property of light controlled isomerization between two different states, the photochromic molecule acts as an inherent basic binary unit to construct all-photonic logic gates.[29,187,191,192] For some photochromic molecules with high thermal stability and fatigue resistance, the information can be reliably stored for a long time and can be multiply write-and-erase cycled. The inherent bi-stability of photoswitches enables them to provide memory storage naturally.[182,184,193-197] In addition, applying a photoswitch in the system opens the possibility of all-photonic operation.[29,32,187]

Compared to the molecular logic systems that require chemical inputs, the all- photonic control excludes any physical access, which enables excellent spatiotemporal control of the system. Moreover, the system becomes waste-free as light does not lead to the build-up of waste products.

To generate variable states, several photoswitches can be synthesized in the same molecule so that the system can respond differently with light of different wavelengths.[29,30] Among various logic devices that are based on photoswitches, sequential logic devices (keypad locks) are highlighted in terms of security and authentication.[177] For sequential logic devices, the states of the output are determined not only by the correct input combination, but also by the order of the applied inputs. The output of the device is switched to the "on" state only if the correct sequence of inputs is given, which corresponds to the procedure of opening the keypad lock. Compared to the combinational logic devices where the states of the output only relied on the input combination, the sequential logic gates are therefore possessing the advantage of stronger user authentication. The functions of sequential logic devices are commonly used in our daily life, such as passwords of different log-in systems, ATM machines and so on.

In our project, the first, basic, sequential molecular logic gate is designed to implement One-time passwords (OTP) generation in combination with two-factor authentication (2FA). The structure of molecular Triad 1 consisting of two fulgimide (FG) and one dithienylethene (DTE) photoswitches is shown in Fig.6.13.

OTP are similar to other types of passwords where the output is sensitive not only to the correct input combination, but also to the order by which the inputs are applied. The difference of OTP compared to other passwords is that the password code generated is "non-static", which are valid for one entry only. The use of OTP dramatically increases the security further, as a stolen password will not break the protected system. In general, OTP is used in combination with two-factor authentication (2FA). The 2FA stands for factors that the user "has" and the user "knows". For example, to login to the bank page, the user needs to "have" the digipass to generate OTP and also "know" the PIN code to access the system.

For the designed system, functions of OTP and 2FA rely on the fluorescent and photochromic properties of Triad 1. The emission of fluorescence from FGc in the FGc–DTEo form of the triad is used as the authentication output. The output is sensitive not only to the correct input combination, but also to the order by which the inputs are applied. The user must "know" the

correct input combination to convert Triad 1 to the fluorescent isomer FGc-DTEo, also the user must have a “key” that refers to the absorption data at 330 nm and 640 nm for authentication.

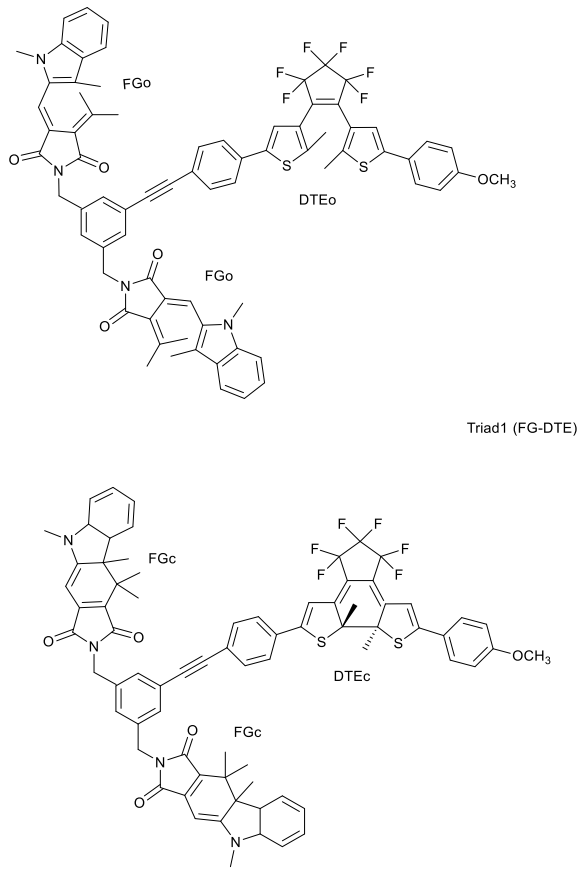

Fig.6.13. Structure scheme of Triad 1. The open and closed forms of fulgimide (FG) are referred to as FGo and FGc, respectively. The DTEo and DTEc stand for the open and the closed form of dithienylethene (DTE), respectively.

The fluorescence of the system can be tuned by two mechanisms, not only by inherent isomerization of photoswitch (between FGo-DTEo and FGc-DTEo) but also by FRET controlled intensity change (between FGc-DTEo and FGc-DTEc). Fig.6.14 shows the isomerization pathways between the 4 different states of Triad 1: FGo-DTEo, FGc-DTEo, FGo-DTEc, and FGc-DTEc. Note that in this representation, both FG units are assumed to adopt the same isomeric form.

In Triad 1, FGo and DTEo can be isomerized with high selectivity to the respective closed isomer. As shown in Fig.6.14, DTEo is preferably isomerized to DTEc by the use of 302 nm light, whereas the optimal wavelength for FGo is 397 nm. 366 nm is used to isomerize both photoswitches to the closed forms. As for the reverse reactions, the FGc-DTEc form is isomerized to FGo-DTEo by green light exposure, whereas red light leads to the formation of FGc-DTEo. The emission of FGc is centered around 630 nm. As there is a large spectral overlap

between the emission of FGc and the absorption of DTEc, the emission of FGc is quenched by FRET in the FGc-DTEc form. Therefore, the only fluorescent state of Triad 1 is FGc-DTEo as the DTE derivative displays no significant emission in any of the two forms.

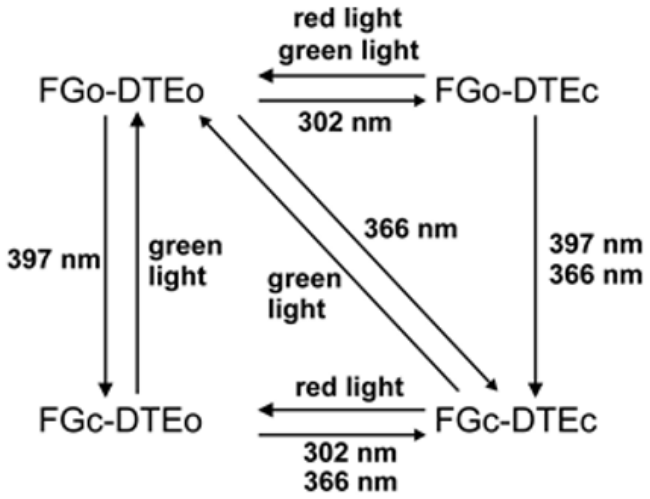

Figure 6.14. Isomerization pathways between the different forms of Triad 1.

The first step to operate the system is to convert the triad from the synthesized FGo-DTEo form to the fluorescent isomer FGc-DTEo. In this case, the user needs to use Triad 1 as a 2-input priority AND gate (PAND gate). The first input is In1=366 nm UV light and the second input is In2=red light, the sequence of which is one of the eight possible ordered input combinations. The output used is fluorescence emission from FGc-DTEo. In this case, the user the must "know" what is ln1 and ln2, also the correct input sequence of them. In this step, the fluorescence of the system is switched "on" by the changes in the inherent fluorescent properties of the FG photoswitch, FGo-DTEo → FGc-DTEo.

After the emission is achieved, the next step is done randomly by the system. Triad 1 can be reset to the initial state FGo-DTEo by green light or converted to non-fluorescent FGc-DTEc by 366 nm UV light. In this step, it can be noticed that the fluorescence of the system can be switched "off" either "inherently" (FGc-DTEo → FGo-DTEo) or by turning "on" the FRET process (FGc-DTEo → FGc-DTEc).

For the final step to get the output that is FG fluorescence, another password needs to be authenticated. In this case, the correct password is different as the case is randomly set by the system. It implies that either the correct "password" is 397 nm exposure (for the FGo-DTEo case) or red light a 623 nm (for the FGc-DTEc case). To know what password to apply, the user must have the "key", which is the absorption data at 330 nm and 640 nm. As it shown in

the Table 6.1, the absorption of FGo-DTEo and FGc-DTEc are different at those two wavelengths. By knowing the key, the user can distinguish the Triad 1 form and input the relevant password.

From here, it can be seen clearly from process that 2FA are fulfilled for the designed molecular logic system. As to get the access, user must "know" the correct input sequence of ln1 and ln2 to convert Triad 1 to the fluorescent isomer FGc-DTEo. Also, for final step, user must "have" the key that refers to the absorption data at 330 nm and 640 nm required for authentication.

Table 6.1. The "key" for OTP required in the 2FA process.

Isomeric form after the "set" operation	Abs. @ 330 nm	Abs. @ 640 nm	Input (password) required for authentication
FGo-DTEo	High	Low	In = 397 nm
FGc-DTEc	Low	High	In = 623 nm

To summarize, in paper IV, the first example of a photoswitch molecular system is designed for the realization of OTP and 2FA. To access the system, the user is required to "know" the right sequence of optical inputs to convert the photochromic Triad 1 to the fluorescent form. Afterwards, OTP of the system is generated based on the isomerized state of Triad 1. To finish the authentication process, the user has to "have" the key for the absorption data at 330 nm and 640 nm. The fluorescence of the system here can be tuned by two mechanisms, either "inherently" by isomerization of the photoswitch, or FRET controlled by controlling the overlap integral between donor emission and acceptor absorption. The obvious drawbacks are of course the limited number of total passwords (two) which implies weak security in the 2FA step (the user has a 50% chance to guess the correct input).

7. Concluding Remarks and Outlook

This thesis presents different approaches to all-photonic control of photochromic systems in which the emission can be either switched between “on” and “off” states or tuned dynamically in a color-correlated fashion. The developed systems can be modulated intrinsically by photoinduced isomerization of photochromic monomers or by photoswitched FRET reactions in donor-acceptor systems. The presented work has potential to be applied in various areas, such as cell studies using fluorescence microscopy, molecular logic and full color reproduction. The all-photonic nature lets the designed systems become non-invasive, waste free, at the same time responding remotely and instantaneously.

In paper I, the DAE derivative Dasy is successfully applied as the sole fluorescent probe where the emission intensity is modulated by red light and the signal is easily filtered out by lock-in detection from any strong fluorescence background. As Dasy has distinct fluorescence in the colorless open isomer and is non-fluorescent in the closed colored form, the fluorescence of Dasy can be easily modulated between two different states through light-induced isomerization processes. Because of its rapid switching capability, Dasy can be modulated with frequencies up to 205 Hz, which is far beyond the typical previous demonstrations (< 1Hz). As the system only depends on isomerization of Dasy monomer without requiring FRET or other excited state communication reactions, the system can be prepared conveniently. The demonstration could be very useful in cell studies and microscopy experiments to avoid disturbance from auto-fluorescence.

In paper II, a molecular cocktail that contains two different DAE derivatives, Dasy and DAE9, is described. It is appealing that the color of the system can be tuned dynamically in a color-correlated fashion only by light-induced isomerization without relying on FRET or other excited state communication processes. In addition, the multi-color cocktail system can be conveniently prepared by mixing two fluorescent DAE derivatives in bulk acetonitrile solution, which avoids the tedious synthesis or any design of complicated supramolecular systems. The color of the system can be continuously changed back and forth by applying UV and visible light, respectively.

To further develop a system with full color reproduction, in paper III, a polymer micelle was used to encapsulate perylene and two photoswitches, DAEg and DAEr. The function of the system can be realized by orthogonally controlled FRET processes between the blue emitting

perylene donor and the two DAE photoswitches that have green and red emission color in the closed form, respectively. The system color is switched from blue to green or blue to red in a color-correlated fashion by selective isomerization of the two photoswitches. It is encouraging to notice all emission colors within the red-green-blue (RGB) area can be generated from one and the same sample by all-photonic stimuli. The system is interesting for many applications, such as luminescent materials and bioimaging.

In paper IV, a sequential molecular logic gate consisting of one dithienylethene (DTE) and two fulgimide (FG) photoswitches was shown to implement one-time passwords generation in combination with two-factor authentication. The fluorescence of the system can be tuned by two mechanisms, either "inherently" by isomerization of the FG photoswitch, or FRET controlled by isomerization of the DTE photoswitch. Although the complexity of the generated password is too low for practical application, we hope the concept will trigger the interests of researchers in the field and be further developed in the future.

The herein described systems can thus change the fluorescent properties by all-photonic stimuli. Although the presented material is to be regarded as proof-of principle, potential applications can be foreseen in mainly fluorescence microscopy. The material presented in paper I shows that fluorescence intensity modulation is feasible using the Dasy monomer, and that this allows for the filtering of undesired background fluorescence. Future studies will target the interface between lock-in-amplification and confocal microscopy to allow for fluorescence imaging using this technique, rather than just the proof-of-principle study in bulk solution presented herein. Moreover, it has been shown that the polymer micelles described in paper III are taken up by live cells. Considering the common problem with spectrally resolving the emission from a collection of fluorescent probes inside live cells, our approach could facilitate this procedure by the demonstrated ability to change the emission color on-demand using light only. Activities along these lines will be undertaken in the future.

8. Acknowledgements

First, I would like to thank you my supervisor Joakim Andréasson for all your support and guidance during my journey at Chalmers. Thanks a lot for being an excellent supervisor and giving me the chance to start my study in Sweden. Also thanks to my co-supervisor Marcus Wilhelmsson, my examiners Per Lincoln and Bo Albinsson.

Nina Kann and Jerker Mårtensson for your care and help as my line managers.

Bo, Vandana, Betül, Fredrik and Jesper for proofreading this thesis.

Shiming, Chien-Wei Hsu, Magnus, Savannah, Wera and Carlos for supporting me with research projects.

Maria, Cassandra, Deise, Wera, Lili, Fredrik, Rasmus, Axel, Pegah, Valeria, Carlos, Jean, Gerard, Long, Andrew, Liam and Andrea thank for the great discussions in the group meetings.

Moa, Anders and Pauline for being my great office mates.

All people at floor 5 for the good atmosphere.

My dear friends from candy office, Elin, Vandana and Betül. Thanks a lot for all of your kind support and happiness giving to me. I feel I am always been cared when you are around.

Alex, Linda, Kristin, Yongjin, Li Gang, Xun qian, Lili, Mi, Xin, Zhiihang, Xin and Zhaojun for your encouragements as my friends. Special thanks to Xin and Zhaojun for all of your company and lovely caring, also Kristin and Linda for your support and guidance on my future pathways.

My dear parents. I love you from the bottom of my heart and miss you so much.

My sweet family, Marcus and Elsa. I am so appreciated to have you here with me. You are the best, my love.

9. References

(1) Bouas‐Laurent, H. D., H., Organic photochromism, *Pure Appl. Chem.* **2001**, 73, 639.

(2) Crano, J. C.; Guglielmetti, R. J. *Organic photochromic and thermochromic compounds*; Kluwer Academic/Plenum Publishers: New York, **1999**.

(3) Irie, M. Diarylethenes for memories and switches. *Chem. Rev.* **2000,** *100* (5), 1685.

(4) Irie, M.; Fukaminato, T.; Matsuda, K.; Kobatake, S. Photochromism of diarylethene molecules and crystals: memories, switches, and actuators. *Chem. Rev.* **2014,** *114* (24), 12174.

(5) Velema, W. A.; Szymanski, W.; Feringa, B. L. Photopharmacology: beyond proof of principle. *J. Am. Chem. Soc.* **2014,** *136* (6), 2178.

(6) Broichhagen, J.; Frank, J. A.; Trauner, D. A roadmap to success in photopharmacology. *Acc. Chem. Res.* **2015,** *48* (7), 1947.

(7) Lerch, M. M.; Hansen, M. J.; van Dam, G. M.; Szymanski, W.; Feringa, B. L. Emerging Targets in Photopharmacology. *Angew. Chem. Int. Ed.* **2016,** *55* (37), 10978.

(8) Szymanski, W.; Beierle, J. M.; Kistemaker, H. A.; Velema, W. A.; Feringa, B. L. Reversible photocontrol of biological systems by the incorporation of molecular photoswitches. *Chem. Rev.* **2013,** *113* (8), 6114.

(9) Nahain, A. A.; Lee, J. E.; Jeong, J. H.; Park, S. Y. Photoresponsive fluorescent reduced graphene oxide by spiropyran conjugated hyaluronic acid for in vivo imaging and target delivery. *Biomacromolecules* **2013,** *14* (11), 4082.

(10) Zhang, J.; Wang, J.; Tian, H. Taking orders from light: progress in photochromic bio-materials. *Mater. Horiz.* **2014,** *1* (2), 169.

(11) Shi, P.; Ju, E.; Yan, Z.; Gao, N.; Wang, J.; Hou, J.; Zhang, Y.; Ren, J.; Qu, X. Spatiotemporal control of cell-cell reversible interactions using molecular engineering. *Nat. Commun.* **2016,** *7*, 13088.

(12) De Poli, M.; Zawodny, W.; Quinonero, O.; Lorch, M.; Webb, S. J.; Clayden, J. Conformational photoswitching of a synthetic peptide foldamer bound within a phospholipid bilayer. *Science* **2016,** *352* (6285), 575.

(13) Reis, S. A.; Ghosh, B.; Hendricks, J. A.; Szantai-Kis, D. M.; Tork, L.; Ross, K. N.; Lamb, J.; Read-Button, W.; Zheng, B.; Wang, H.et al. Light-controlled modulation of gene expression by chemical optoepigenetic probes. *Nat. Chem. Biol.* **2016,** *12* (5), 317.

(14) Zhang, J.; Fu, Y.; Han, H. H.; Zang, Y.; Li, J.; He, X. P.; Feringa, B. L.; Tian, H. Remote light-controlled intracellular target recognition by photochromic fluorescent glycoprobes. *Nat. Commun.* **2017,** *8* (1), 987.

(15) Deng, M.; Zhang, Y.; Wang, Y.; Jiang, S. Polymeric nanoparticles based on CDs with photoreversible dual-color fluorescence modulation. *J. Mater. Chem. C* **2020,** *8* (44), 15697.

(16) Qiang, Z.; Shebek, K. M.; Irie, M.; Wang, M. A Polymerizable Photoswitchable Fluorophore for Super-Resolution Imaging of Polymer Self-Assembly and Dynamics. *ACS Macro Lett.* **2018,** *7* (12), 1432.

(17) Nevskyi, O.; Sysoiev, D.; Dreier, J.; Stein, S. C.; Oppermann, A.; Lemken, F.; Janke, T.; Enderlein, J.; Testa, I.; Huhn, T.et al. Fluorescent Diarylethene Photoswitches-A Universal Tool for Super-Resolution Microscopy in Nanostructured Materials. *Small* **2018,** *14* (10).

(18) Nevskyi, O.; Sysoiev, D.; Oppermann, A.; Huhn, T.; Woll, D. Nanoscopic Visualization of Soft Matter Using Fluorescent Diarylethene Photoswitches. *Angew. Chem. Int. Ed.* **2016,** *55* (41), 12698.

(19) Uno, K.; Bossi, M. L.; Konen, T.; Belov, V. N.; Irie, M.; Hell, S. W. Asymmetric Diarylethenes with Oxidized 2‐Alkylbenzothiophen‐3‐yl Units: Chemistry, Fluorescence, and Photoswitching. *Adv. Opt. Mater.* **2019,** *7* (6).

(20) Roubinet, B.; Weber, M.; Shojaei, H.; Bates, M.; Bossi, M. L.; Belov, V. N.; Irie, M.; Hell, S. W. Fluorescent Photoswitchable Diarylethenes for Biolabeling and Single-Molecule Localization Microscopies with Optical Superresolution. *J. Am. Chem. Soc.* **2017,** *139* (19), 6611.

(21) Roubinet, B.; Bossi, M. L.; Alt, P.; Leutenegger, M.; Shojaei, H.; Schnorrenberg, S.; Nizamov, S.; Irie, M.; Belov, V. N.; Hell, S. W. Carboxylated Photoswitchable Diarylethenes for Biolabeling and Super-Resolution RESOLFT Microscopy. *Angew. Chem. Int. Ed.* **2016,** *55* (49), 15429.

(22) Wöll, D.; Flors, C. Super-resolution Fluorescence Imaging for Materials Science. *Small Methods* **2017,** *1* (10).

(23) Tian, Z.; Li, A. D. Photoswitching-enabled novel optical imaging: innovative solutions for real-world challenges in fluorescence detections. *Acc. Chem. Res.* **2013,** *46* (2), 269.

(24) Naren, G.; Hsu, C. W.; Li, S.; Morimoto, M.; Tang, S.; Hernando, J.; Guirado, G.; Irie, M.; Raymo, F. M.; Sunden, H.et al. An all-photonic full color RGB system based on molecular photoswitches. *Nat. Commun.* **2019,** *10* (1), 3996.

(25) Bu, J.; Watanabe, K.; Hayasaka, H.; Akagi, K. Photochemically colour-tuneable white fluorescence illuminants consisting of conjugated polymer nanospheres. *Nat. Commun.* **2014,** *5*, 3799.

(26) Yu, M.; Zhang, P.; Krishnan, B. P.; Wang, H.; Gao, Y.; Chen, S.; Zeng, R.; Cui, J.; Chen, J. From a Molecular Toolbox to a Toolbox for Photoswitchable Fluorescent Polymeric Nanoparticles. *Adv. Funct. Mater.* **2018,** *28* (46).

(27) Hou, L.; Zhang, X.; Cotella, G. F.; Carnicella, G.; Herder, M.; Schmidt, B. M.; Pätzel, M.; Hecht, S.; Cacialli, F.; Samorì, P. Optically switchable organic light-emitting transistors. *Nat. Nanotechnol.* **2019,** *14* (4), 347.

(28) Xu, Z.; Liu, Q. T.; Wang, X.; Liu, Q.; Hean, D.; Chou, K. C.; Wolf, M. O. Quinoline-containing diarylethenes: bridging between turn-on fluorescence, RGB switching and room temperature phosphorescence. *Chem. Sci.* **2020,** *11* (10), 2729.

(29) Andréasson, J.; Pischel, U.; Straight, S. D.; Moore, T. A.; Moore, A. L.; Gust, D. All-photonic multifunctional molecular logic device. *J. Am. Chem. Soc.* **2011,** *133* (30), 11641.

(30) Ai, Q.; Ahn, K.-H. A photoswitchable diarylethene heterodimer for use as a multifunctional logic gate. *RSC Adv.* **2016,** *6* (49), 43000.

(31) Johnstone, M. D.; Hsu, C. W.; Hochbaum, N.; Andréasson, J.; Sunden, H. Multi-color emission with orthogonal input triggers from a diarylethene pyrene-OTHO organogelator cocktail. *Chem. Commun.* **2020,** *56* (6), 988.

(32) Kim, D.; Kim, J.; Lee, T. S. Photoswitchable chromic behavior of conjugated polymer films for reversible patterning and construction of a logic gate. *Polym. Chem.* **2017,** *8* (36), 5539.

(33) Singh, A.; Verma, P.; Laha, S.; Samanta, D.; Roy, S.; Maji, T. K. Photochromic Conjugated Microporous Polymer Manifesting Bio-Inspired pcFRET and Logic Gate Functioning. *ACS Appl. Mater. Interfaces* **2020,** *12* (18), 20991.

(34) Li, Y.; Chen, X.; Weng, T.; Yang, J.; Zhao, C.; Wu, B.; Zhang, M.; Zhu, L.; Zou, Q. A monomolecular platform with varying gated photochromism. *RSC Adv.* **2020,** *10* (69), 42194.

(35) Liao, G.; Zheng, C.; Xue, D.; Fan, C.; Liu, G.; Pu, S. A diarylethene-based fluorescent chemosensor for the sequential recognition of Fe3+ and cysteine. *RSC Adv.* **2016,** *6* (41), 34748.

(36) Zhang, J.; Tian, H. The Endeavor of Diarylethenes: New Structures, High Performance, and Bright Future. *Adv. Opt. Mater.* **2018,** *6* (6).

(37) Fukaminato, T.; Ishida, S.; Métivier, R. Photochromic fluorophores at the molecular and nanoparticle levels: fundamentals and applications of diarylethenes. *NPG Asia Mater.* **2018,** *10* (9), 859.

(38) Uno, K.; Niikura, H.; Morimoto, M.; Ishibashi, Y.; Miyasaka, H.; Irie, M. In situ preparation of highly fluorescent dyes upon photoirradiation. *J. Am. Chem. Soc.* **2011,** *133* (34), 13558.

(39) Chibisov, A. K.; Gorner, H. Photoprocesses in spiropyran-derived merocyanines. *J. Phys. Chem. A* **1997,** *101* (24), 4305.

(40) Liang, Y. C.; Dvornikov, A. S.; Rentzepis, P. M. Synthesis and photochemistry of photochromic fluorescing indol-2-ylfulgimides. *J. Mater. Chem.* **2000,** *10* (11), 2477.

(41) Ishida, S.; Fukaminato, T.; Kitagawa, D.; Kobatake, S.; Kim, S.; Ogata, T.; Kurihara, S. Wavelength-selective and high-contrast multicolour fluorescence photoswitching in a mixture of photochromic nanoparticles. *Chem. Commun.* **2017,** *53* (59), 8268.

(42) Kim, D.; Park, S. Y. Multicolor Fluorescence Photoswitching: Color-Correlated versus Color-Specific Switching. *Adv. Opt. Mater.* **2018,** *6* (20).

(43) Uno, K.; Bossi, M. L.; Belov, V. N.; Irie, M.; Hell, S. W. Multicolour fluorescent "sulfide-sulfone" diarylethenes with high photo-fatigue resistance. *Chem. Commun.* **2020,** *56* (14), 2198.

(44) Folling, J.; Polyakova, S.; Belov, V.; van Blaaderen, A.; Bossi, M. L.; Hell, S. W. Synthesis and characterization of photoswitchable fluorescent silica nanoparticles. *Small* **2008,** *4* (1), 134.

(45) Zhu, L.; Wu, W.; Zhu, M. Q.; Han, J. J.; Hurst, J. K.; Li, A. D. Reversibly photoswitchable dual-color fluorescent nanoparticles as new tools for live-cell imaging. *J. Am. Chem. Soc.* **2007,** *129* (12), 3524.

(46) Kim, D.; Kwon, J. E.; Park, S. Y. Fully Reversible Multistate Fluorescence Switching: Organogel System Consisting of Luminescent Cyanostilbene and Turn-On Diarylethene. *Adv. Funct. Mater.* **2018,** *28*.

(47) Kim, S.; Yoon, S. J.; Park, S. Y. Highly fluorescent chameleon nanoparticles and polymer films: multicomponent organic systems that combine FRET and photochromic switching. *J. Am. Chem. Soc.* **2012,** *134* (29), 12091.

(48) Copley, G.; Gillmore, J. G.; Crisman, J.; Kodis, G.; Gray, C. L.; Cherry, B. R.; Sherman, B. D.; Liddell, P. A.; Paquette, M. M.; Kelbauskas, L.et al. Modulating Short Wavelength Fluorescence with Long Wavelength Light. *Journal of the American Chemical Society* **2014,** *136* (34), 11994.

(49) Naren, G.; Larsson, W.; Benitez-Martin, C.; Li, S.; Perez-Inestrosa, E.; Albinsson, B.; Andréasson, J. Rapid amplitude-modulation of a diarylethene photoswitch: en route to contrast-enhanced fluorescence imaging. *Chem. Sci.* **2021,** *12* (20), 7073.

(50) Naren, G.; Li, S.; Andréasson, J. A simplicity-guided cocktail approach toward multicolor fluorescent systems. *Chem. Commun.* **2020,** *56* (23), 3377.

(51) Lakowicz, J. R. *Principles of fluorescence spectroscopy*; 3rd ed.; Springer: New York, **2006.**

(52) CIE, C.; Commission Internationale de l'Eclairage Proceedings, Cambridge University Press, Cambridge, **1931**.

(53) Acdx; The CIE 1931 XYZ color matching functions. https://commons.wikimedia.org/wiki/File:CIE_1931_XYZ_Color_Matching_Functions.svg, File:CIE1931 XYZCMF.png, no change made. Wikimedia Commons, **2009**.

(54) Kurokawa, Y.; Hayakawa, R.; Shimada, S.; Tanaka, K.; Higashiguchi, K.; Noguchi, Y.; Matsuda, K.; Wakayama, Y. Photocontrollable ambipolar transistors with π-conjugated diarylethene photochromic channels. *Japanese Journal of Applied Physics* **2019,** *58* (SD).

(55) Börjesson, K.; Herder, M.; Grubert, L.; Duong, D. T.; Salleo, A.; Hecht, S.; Orgiu, E.; Samorì, P. Optically switchable transistors comprising a hybrid photochromic molecule/n-type organic active layer. *J. Mater. Chem. C* **2015,** *3* (16), 4156.

(56) Leydecker, T.; Herder, M.; Pavlica, E.; Bratina, G.; Hecht, S.; Orgiu, E.; Samori, P. Flexible non-volatile optical memory thin-film transistor device with over 256 distinct levels based on an organic bicomponent blend. *Nat. Nanotechnol.* **2016,** *11* (9), 769.

(57) Gemayel, M. E.; Borjesson, K.; Herder, M.; Duong, D. T.; Hutchison, J. A.; Ruzie, C.; Schweicher, G.; Salleo, A.; Geerts, Y.; Hecht, S.et al. Optically switchable transistors by simple incorporation of photochromic systems into small-molecule semiconducting matrices. *Nat. Commun.* **2015,** *6*, 6330.

(58) Hayakawa, R.; Higashiguchi, K.; Matsuda, K.; Chikyow, T.; Wakayama, Y. Optically and electrically driven organic thin film transistors with diarylethene photochromic channel layers. *ACS Appl. Mater. Interfaces* **2013,** *5* (9), 3625.

(59) Orgiu, E.; Crivillers, N.; Herder, M.; Grubert, L.; Patzel, M.; Frisch, J.; Pavlica, E.; Duong, D. T.; Bratina, G.; Salleo, A.et al. Optically switchable transistor via energy-level phototuning in a bicomponent organic semiconductor. *Nat. Chem.* **2012,** *4* (8), 675.

(60) Nikolayenko, V. I.; Herbert, S. A.; Barbour, L. J. Reversible structural switching of a metal-organic framework by photoirradiation. *Chem. Commun.* **2017,** *53* (81), 11142.

(61) Han, M.; Michel, R.; He, B.; Chen, Y. S.; Stalke, D.; John, M.; Clever, G. H. Light-triggered guest uptake and release by a photochromic coordination cage. *Angew. Chem. Int. Ed.* **2013,** *52* (4), 1319.

(62) Fan, C. B.; Le Gong, L.; Huang, L.; Luo, F.; Krishna, R.; Yi, X. F.; Zheng, A. M.; Zhang, L.; Pu, S. Z.; Feng, X. F.et al. Significant Enhancement of C2 H2 /C2 H4 Separation by a Photochromic Diarylethene Unit: A Temperature- and Light-Responsive Separation Switch. *Angew. Chem. Int. Ed.* **2017,** *56* (27), 7900.

(63) Zheng, Y.; Sato, H.; Wu, P.; Jeon, H. J.; Matsuda, R.; Kitagawa, S. Flexible interlocked porous frameworks allow quantitative photoisomerization in a crystalline solid. *Nat. Commun.* **2017,** *8* (1), 100.

(64) Park, J.; Yuan, D.; Pham, K. T.; Li, J. R.; Yakovenko, A.; Zhou, H. C. Reversible alteration of CO2 adsorption upon photochemical or thermal treatment in a metal-organic framework. *J. Am. Chem. Soc.* **2012,** *134* (1), 99.

(65) Modrow, A.; Zargarani, D.; Herges, R.; Stock, N. The first porous MOF with photoswitchable linker molecules. *Dalton Trans.* **2011,** *40* (16), 4217.

(66) Jones, C. D.; Steed, J. W. Gels with sense: supramolecular materials that respond to heat, light and sound. *Chem. Soc. Rev.* **2016,** *45* (23), 6546.

(67) Draper, E. R.; Adams, D. J. Photoresponsive gelators. *Chem. Commun.* **2016,** *52* (53), 8196.

(68) Zhang, X.; Hou, L.; Samori, P. Coupling carbon nanomaterials with photochromic molecules for the generation of optically responsive materials. *Nat. Commun.* **2016,** *7*, 11118.

(69) Andréasson, J.; Pischel, U. Molecules with a sense of logic: a progress report. *Chem. Soc. Rev.* **2015,** *44* (5), 1053.

(70) Orgiu, E.; Samori, P. 25th anniversary article: organic electronics marries photochromism: generation of multifunctional interfaces, materials, and devices. *Adv. Mater.* **2014,** *26* (12), 1827.

(71) Nie, H.; Self, J. L.; Kuenstler, A. S.; Hayward, R. C.; Read de Alaniz, J. Multiaddressable Photochromic Architectures: From Molecules to Materials. *Adv. Opt. Mater.* **2019,** *7* (16).

(72) Jin, K.; Ji, X.; Yang, T.; Zhang, J.; Tian, W.; Yu, J.; Zhang, X.; Chen, Z.; Zhang, J. Facile access to photo-switchable, dynamic-optical, multi-colored and solid-state materials from carbon dots and cellulose for photo-rewritable paper and advanced anti-counterfeiting. *Chem. Eng. J.* **2021,** *406*.

(73) Erbas-Cakmak, S.; Kolemen, S.; Sedgwick, A. C.; Gunnlaugsson, T.; James, T. D.; Yoon, J.; Akkaya, E. U. Molecular logic gates: the past, present and future. *Chem. Soc. Rev.* **2018,** *47* (7), 2228.

(74) Bleger, D.; Hecht, S. Visible-Light-Activated Molecular Switches. *Angew. Chem. Int. Ed.* **2015,** *54* (39), 11338.

(75) Hatano, S.; Horino, T.; Tokita, A.; Oshima, T.; Abe, J. Unusual negative photochromism via a short-lived imidazolyl radical of 1,1'-binaphthyl-bridged imidazole dimer. *J. Am. Chem. Soc.* **2013,** *135* (8), 3164.

(76) Yamaguchi, T.; Maity, A.; Polshettiwar, V.; Ogawa, M. Negative Photochromism Based on Molecular Diffusion between Hydrophilic and Hydrophobic Particles in the Solid State. *Inorg. Chem.* **2018,** *57* (7), 3671.

(77) Irie, M. *Diarylethene Molecular Photoswitches Concepts and Functionalities*; Wiley-VCH, Weinheim, **2021**.

(78) Kothapalli, S. S. K.; Kannekanti, V. K.; Ye, Z.; Yang, Z.; Chen, L.; Cai, Y.; Zhu, B.; Feng, W.; Yuan, L. Light-controlled switchable complexation by a non-photoresponsive hydrogen-bonded amide macrocycle. *Org. Chem. Front.* **2020,** *7* (6), 846.

(79) Wimberger, L.; Prasad, S. K. K.; Peeks, M. D.; Andréasson, J.; Schmidt, T. W.; Beves, J. E. Large, Tunable, and Reversible pH Changes by Merocyanine Photoacids. *J Am Chem Soc* **2021,** *143* (49), 20758.

(80) Stranius, K.; Borjesson, K. Determining the Photoisomerization Quantum Yield of Photoswitchable Molecules in Solution and in the Solid State. *Sci. Rep.* **2017,** *7*, 41145.

(81) Brouwer, A. M. Standards for photoluminescence quantum yield measurements in solution (IUPAC Technical Report). *Pure Appl. Chem.* **2011,** *83* (12), 2213.

(82) Hell, S. W. Microscopy and its focal switch. *Nat. Methods* **2009,** *6* (1), 24.

(83) Hell, S. W. Far-field optical nanoscopy. *Science* **2007,** *316* (5828), 1153.

(84) Zhang, Z.; Wang, W.; Jin, P.; Xue, J.; Sun, L.; Huang, J.; Zhang, J.; Tian, H. A building-block design for enhanced visible-light switching of diarylethenes. *Nat. Commun.* **2019,** *10* (1).

(85) Feng, G.; Ding, D.; Li, K.; Liu, J.; Liu, B. Reversible photoswitching conjugated polymer nanoparticles for cell and ex vivo tumor imaging. *Nanoscale* **2014,** *6* (8), 4141.

(86) Yang, T.; Liu, Q.; Li, J.; Pu, S.; Yang, P.; Li, F. Photoswitchable upconversion nanophosphors for small animal imaging in vivo. *RSC Adv.* **2014,** *4* (30).

(87) Wu, T.; Johnsen, B.; Qin, Z.; Morimoto, M.; Baillie, D.; Irie, M.; Branda, N. R. Two-colour fluorescent imaging in organisms using self-assembled nano-systems of upconverting nanoparticles and molecular switches. *Nanoscale* **2015,** *7* (26), 11263.

(88) Kuo, C. T.; Thompson, A. M.; Gallina, M. E.; Ye, F.; Johnson, E. S.; Sun, W.; Zhao, M.; Yu, J.; Wu, I. C.; Fujimoto, B.et al. Optical painting and fluorescence activated sorting of single adherent cells labelled with photoswitchable Pdots. *Nat Commun* **2016,** *7*, 11468.

(89) Osakada, Y.; Fukaminato, T.; Ichinose, Y.; Fujitsuka, M.; Harada, Y.; Majima, T. Live Cell Imaging Using Photoswitchable Diarylethene-Doped Fluorescent Polymer Dots. *Chem. Asian J.* **2017,** *12* (20), 2660.

(90) Nakamura, S.; Irie, M. Thermally irreversible photochromic systems. A theoretical study. *J. Org. Chem.* **1988,** *53* (26), 6136.

(91) Uchida, K.; Tsuchida, E.; Aoi, Y.; Nakamura, S.; Irie, M. Substitution Effect on the Coloration Quantum Yield of a Photochromic Bisbenzothienylethene. *Chem. Lett.* **1999,** *28* (1), 63.

(92) Yamaguchi, T.; Irie, M. Photochromism of bis(2-alkyl-1-benzothiophen-3-yl)perfluorocyclopentene derivatives. *J. Photochem. Photobiol.* **2006,** *178* (2-3), 162.

(93) Ohsumi, M.; Hazama, M.; Fukaminato, T.; Irie, M. Photocyclization reaction of a diarylmaleimide derivative in polar solvents. *Chem. Commun.* **2008**, DOI:10.1039/b802780c 10.1039/b802780c(28).

(94) Irie, M.; Sayo, K. Solvent effects on the photochromic reactions of diarylethene derivatives. *J. Phys. Chem.* **2002,** *96* (19), 7671.

(95) Morimoto, M.; Takagi, Y.; Hioki, K.; Nagasaka, T.; Sotome, H.; Ito, S.; Miyasaka, H.; Irie, M. A turn-on mode fluorescent diarylethene: Solvatochromism of fluorescence. *Dyes Pigm.* **2018,** *153*, 144.

(96) Gillanders, F.; Giordano, L.; Díaz, S. A.; Jovin, T. M.; Jares-Erijman, E. A. Photoswitchable fluorescent diheteroarylethenes: substituent effects on photochromic and solvatochromic properties. *Photochem. Photobiol. Sci.* **2014,** *13* (3).

(97) Shibata, K.; Kuroki, L.; Fukaminato, T.; Irie, M. Fluorescence Switching of a Diarylethene Derivative Having Oxazole Rings. *Chem. Lett.* **2008,** *37* (8), 832.

(98) Yan, Y.; Petchprayoon, C.; Mao, S.; Marriott, G. Reversible optical control of cyanine fluorescence in fixed and living cells: optical lock-in detection immunofluorescence imaging microscopy. *Philos. Trans. R. Soc. B* **2013,** *368* (1611), 20120031.

(99) Tian, Z.; Wu, W.; Wan, W.; Li, A. D. Photoswitching-induced frequency-locked donor-acceptor fluorescence double modulations identify the target analyte in complex environments. *J. Am. Chem. Soc.* **2011,** *133* (40), 16092.

(100) Marriott, G.; Mao, S.; Sakata, T.; Ran, J.; Jackson, D. K.; Petchprayoon, C.; Gomez, T. J.; Warp, E.; Tulyathan, O.; Aaron, H. L.et al. Optical lock-in detection imaging microscopy for contrast-enhanced imaging in living cells. *Proc. Natl. Acad. Sci. U.S.A.* **2008,** *105* (46), 17789.

(101) Abbandonato, G.; Storti, B.; Signore, G.; Beltram, F.; Bizzarri, R. Quantitative optical lock-in detection for quantitative imaging of switchable and non-switchable components. *Microsc. Res. Tech.* **2016,** *79* (10), 929.

(102) Mannuzzu, L. M.; Moronne, M. M.; Isacoff, E. Y. Direct physical measure of conformational rearrangement underlying potassium channel gating. *Science* **1996,** *271* (5246), 213.

(103) Yan, Y.; Marriott, M. E.; Petchprayoon, C.; Marriott, G. Optical switch probes and optical lock-in detection (OLID) imaging microscopy: high-contrast fluorescence imaging within living systems. *Biochem. J.* **2011,** *433* (3), 411.

(104) Petchprayoon, C.; Yan, Y.; Mao, S.; Marriott, G. Rational design, synthesis, and characterization of highly fluorescent optical switches for high-contrast optical lock-in detection (OLID) imaging microscopy in living cells. *Bioorg. Med. Chem.* **2011,** *19* (3), 1030.

(105) Mao, S.; Benninger, R. K.; Yan, Y.; Petchprayoon, C.; Jackson, D.; Easley, C. J.; Piston, D. W.; Marriott, G. Optical lock-in detection of FRET using synthetic and genetically encoded optical switches. *Biophys. J.* **2008,** *94* (11), 4515.

(106) Wang, Y.; Wu, L.; Dai, Y.; Jiang, X.; Petchprayoon, C.; Lee, J. E.; Jiang, T.; Yan, Y.; Marriott, G. High-Contrast Fluorescence Imaging in Fixed and Living Cells Using Optimized Optical Switches. *PLoS One* **2013,** *8* (6).

(107) Jeong, Y.-C.; Park, D. G.; Lee, I. S.; Yang, S. I.; Ahn, K.-H. Highly fluorescent photochromic diarylethene with an excellent fatigue property. *J. Mater. Chem.* **2009,** *19* (1), 97.

(108) Hsu, C. W.; Sauvee, C.; Sunden, H.; Andréasson, J. Writing and erasing multicolored information in diarylethene-based supramolecular gels. *Chem. Sci.* **2018,** *9* (41), 8019.

(109) Wu, H.; Chen, Y.; Dai, X.; Li, P.; Stoddart, J. F.; Liu, Y. In Situ Photoconversion of Multicolor Luminescence and Pure White Light Emission Based on Carbon Dot-Supported Supramolecular Assembly. *J. Am. Chem. Soc.* **2019,** *141* (16), 6583.

(110) Andréasson, J.; Pischel, U. Molecules for security measures: from keypad locks to advanced communication protocols. *Chem. Soc. Rev.* **2018,** *47* (7), 2266.

(111) Diaz, S. A.; Giordano, L.; Azcarate, J. C.; Jovin, T. M.; Jares-Erijman, E. A. Quantum dots as templates for self-assembly of photoswitchable polymers: small, dual-color nanoparticles capable of facile photomodulation. *J. Am. Chem. Soc.* **2013,** *135* (8), 3208.

(112) Zhang, Y.; Zhang, K.; Wang, J.; Tian, Z.; Li, A. D. Photoswitchable fluorescent nanoparticles and their emerging applications. *Nanoscale* **2015,** *7* (46), 19342.

(113) Tian, Z.; Wu, W.; Wan, W.; Li, A. D. Single-chromophore-based photoswitchable nanoparticles enable dual-alternating-color fluorescence for unambiguous live cell imaging. *J. Am. Chem. Soc.* **2009,** *131* (12), 4245.

(114) Qu, D. H.; Wang, Q. C.; Zhang, Q. W.; Ma, X.; Tian, H. Photoresponsive Host-Guest Functional Systems. *Chem. Rev.* **2015,** *115* (15), 7543.

(115) Bälter, M.; Li, S.; Morimoto, M.; Tang, S.; Hernando, J.; Guirado, G.; Irie, M.; Raymo, F. M.; Andréasson, J. Emission color tuning and white-light generation based on photochromic control of energy transfer reactions in polymer micelles. *Chem. Sci.* **2016,** *7* (9), 5867.

(116) Zhong, W.; Zeng, X.; Chen, J.; Hong, Y.; Xiao, L.; Zhang, P. Photoswitchable fluorescent polymeric nanoparticles for rewritable fluorescence patterning and intracellular dual-color imaging with AIE-based fluorogens as FRET donors. *Polymer Chemistry* **2017,** *8* (33), 4849.

(117) Keyvan Rad, J.; Mahdavian, A. R. Photoswitchable dual-color fluorescent particles from seeded emulsion polymerization and role of some affecting parameters on FRET process. *European Polymer Journal* **2017,** *88*, 56.

(118) Chen, J.; Zhong, W.; Xue, M.; Wang, H.; Yu, M.; Zhang, P.; Yi, P. Photochromic RAFT reagent helps construct superior photoswitchable fluorescent polymer nanoparticles for rewritable fluorescence patterning and intracellular dual-color imaging. *Polym. Chem.* **2017,** *8* (42), 6520.

(119) Chen, Q.; Zhang, D.; Zhang, G.; Yang, X.; Feng, Y.; Fan, Q.; Zhu, D. Multicolor Tunable Emission from Organogels Containing Tetraphenylethene, Perylenediimide, and Spiropyran Derivatives. *Adv. Funct. Mater.* **2010,** *20* (19), 3244.

(120) Tian, W.; Zhang, J.; Yu, J.; Wu, J.; Zhang, J.; He, J.; Wang, F. Phototunable Full-Color Emission of Cellulose-Based Dynamic Fluorescent Materials. *Adv. Funct. Mater.* **2018,** *28* (9).

(121) Dryza, V.; Smith, T. A.; Bieske, E. J. Blue to near-IR energy transfer cascade within a dye-doped polymer matrix, mediated by a photochromic molecular switch. *Phys. Chem. Chem. Phys.* **2016,** *18* (7), 5095.

(122) Ritchie, C.; Vamvounis, G.; Soleimaninejad, H.; Smith, T. A.; Bieske, E. J.; Dryza, V. Photochrome-doped organic films for photonic keypad locks and multi-state fluorescence. *Phys. Chem. Chem. Phys.* **2017,** *19* (30), 19984.

(123) Wang, S.; Li, T.; Zhang, X.; Ma, L.; Li, C.; Yao, X.; Cao, D.; Ma, X. Stimuli‐Responsive Copolymer and Uniform Polymeric Nanoparticles with Photochromism and Switchable Emission. *ChemPhotoChem.* **2019,** *3* (7), 568.

(124) Lin, Z.; Wang, H.; Yu, M.; Guo, X.; Zhang, C.; Deng, H.; Zhang, P.; Chen, S.; Zeng, R.; Cui, J.et al. Photoswitchable ultrahigh-brightness red fluorescent polymeric nanoparticles for information encryption, anti-counterfeiting and bioimaging. *J. Mater. Chem. C* **2019,** *7* (37), 11515.

(125) Wang, H.; Zhang, P.; Krishnan, B. P.; Yu, M.; Liu, J.; Xue, M.; Chen, S.; Zeng, R.; Cui, J.; Chen, J. Switchable single fluorescent polymeric nanoparticles for stable white-light generation. *J. Mater. Chem. C* **2018,** *6* (37), 9897.

(126) Watanabe, K.; Hayasaka, H.; Miyashita, T.; Ueda, K.; Akagi, K. Dynamic Control of Full-Colored Emission and Quenching of Photoresponsive Conjugated Polymers by Photostimuli. *Adv. Funct. Mater.* **2015,** *25* (19), 2794.

(127) Ma, J.; Cui, X. N.; Wang, F.; Wu, X. Y.; Zhao, J. Z.; Li, X. W. Photoswitching of the Triplet Excited State of DiiodoBodipy-Dithienylethene Triads and Application in Photo-Controllable Triplet-Triplet Annihilation Upconversion. *J. Org. Chem.* **2014,** *79* (22), 10855.

(128) Xu, K. J.; Zhao, J. Z.; Cui, X. N.; Ma, J. Switching of the Triplet Triplet-Annihilation Upconversion with Photoresponsive Triplet Energy Acceptor: Photocontrollable Singlet/Triplet Energy Transfer and Electron Transfer. *J. Phys. Chem. A* **2015,** *119* (3), 468.

(129) Thurn, J.; Maier, J.; Pars, M.; Graf, K.; Thelakkat, M.; Kohler, J. Temperature dependence of the conversion efficiency of photochromic perylene bisimide dithienylcyclopentene triads embedded in a polymer. *Phys. Chem. Chem. Phys.* **2017,** *19* (38), 26065.

(130) Maier, J.; Pars, M.; Weller, T.; Thelakkat, M.; Kohler, J. Deliberate Switching of Single Photochromic Triads. *Sci. Rep.* **2017,** *7*.

(131) Irie, M.; Fukaminato, T.; Sasaki, T.; Tamai, N.; Kawai, T. Organic chemistry: A digital fluorescent molecular photoswitch. *Nature* **2002,** *420* (6917), 759.

(132) Jeong, K.; Park, S.; Lee, Y. D.; Lim, C. K.; Kim, J.; Chung, B. H.; Kwon, I. C.; Park, C. R.; Kim, S. Conjugated Polymer/Photochromophore Binary Nanococktails: Bistable Photoswitching of Near-Infrared Fluorescence for In Vivo Imaging. *Adv. Mater.* **2013,** *25* (39), 5574.

(133) Jung, H. Y.; You, S.; Lee, C.; You, S.; Kim, Y. One-pot synthesis of monodispersed silica nanoparticles for diarylethene-based reversible fluorescence photoswitching in living cells. *Chem. Commun.* **2013,** *49* (68), 7528.

(134) Yagai, S.; Ishiwatari, K.; Lin, X.; Karatsu, T.; Kitamura, A.; Uemura, S. Rational Design of Photoresponsive Supramolecular Assemblies Based on Diarylethene. *Chem. Eur. J.* **2013,** *19* (22), 6971.

(135) Samanta, S. K.; Bhattacharya, S. Excellent chirality transcription in two-component photochromic organogels assembled through J-aggregation. *Chem. Commun.* **2013,** *49* (14), 1425.

(136) Wei, S. C.; Pan, M.; Li, K.; Wang, S. J.; Zhang, J. Y.; Su, C. Y. A Multistimuli-Responsive Photochromic Metal-Organic Gel. *Adv. Mater.* **2014,** *26* (13), 2072.

(137) Wu, H.; Chen, Y.; Liu, Y. Reversibly Photoswitchable Supramolecular Assembly and Its Application as a Photoerasable Fluorescent Ink. *Adv. Mater.* **2017,** *29* (10).

(138) Cheng, H. B.; Zhang, H. Y.; Liu, Y. Dual-Stimulus Luminescent Lanthanide Molecular Switch Based on an Unsymmetrical Diarylperfluorocyclopentene. *J. Am. Chem. Soc.* **2013,** *135* (28), 10190.

(139) Fukaminato, T.; Sasaki, T.; Kawai, T.; Tamai, N.; Irie, M. Digital photoswitching of fluorescence based on the photochromism of diarylethene derivatives at a single-molecule level. *J. Am. Chem. Soc.* **2004,** *126* (45), 14843.

(140) Berberich, M.; Krause, A. M.; Orlandi, M.; Scandola, F.; Wurthner, F. Toward fluorescent memories with nondestructive readout: Photoswitching of fluorescence by intramolecular electron transfer in a diaryl ethene-perylene bisimide photochromic system. *Angew. Chem. Int. Ed.* **2008,** *47* (35), 6616.

(141) Bu, J. X.; Watanabe, K.; Hayasaka, H.; Akagi, K. Photochemically colour-tuneable white fluorescence illuminants consisting of conjugated polymer nanospheres. *Nature Communications* **2014,** *5*.

(142) Mo, S. Z.; Meng, Q. T.; Wan, S. L.; Su, Z. Q.; Yan, H.; Tang, B. Z.; Yin, M. Z. Tunable Mechanoresponsive Self-Assembly of an Amide-Linked Dyad with Dual Sensitivity of Photochromism and Mechanochromism. *Adv. Funct. Mater.* **2017,** *27* (28).

(143) Lee, S. H.; Bui, H. T.; Vales, T. P.; Cho, S.; Kim, H. J. Multi-color fluorescence of pNIPAM-Based nanogels modulated by dual stimuli-responsive FRET processes. *Dyes Pigm.* **2017,** *145*, 216.

(144) Liao, B.; Wang, W.; Long, P.; Deng, X. T.; He, B. Q.; Liu, Q. Q.; Yi, S. J. The carbon nanoparticles grafted with copolymers of styrene and spiropyran with reversibly photoswitchable fluorescence. *Carbon* **2015,** *91*, 30.

(145) Rad, J. K.; Mahdavian, A. R.; Khoei, S.; Esfahani, A. J. FRET-based acrylic nanoparticles with dual-color photoswitchable properties in DU145 human prostate cancer cell line labeling. *Polymer* **2016,** *98*, 263.

(146) Achilleos, D. S.; Hatton, T. A.; Vamvakaki, M. Photoreponsive Hybrid Nanoparticles with Inherent FRET Activity. *Langmuir* **2016,** *32* (23), 5981.

(147) Liao, B.; Lv, H.; Deng, X. T.; He, B. Q.; Liu, Q. Q. Spiropyran-modified silicon quantum dots with reversibly switchable photoluminescence. *J. Nanoparticle Res.* **2017,** *19* (8).

(148) Kim, D.; Lee, T. S. Photoswitchable Emission Color Change in Nanodots Containing Conjugated Polymer and Photochrome. *ACS Appl. Mater. Interfaces* **2016,** *8* (50), 34770.

(149) Kim, D.; Kwon, J. E.; Park, S. Y. Is Color-Specific Photoswitching in Dual-Color Fluorescence Systems Possible? Manipulating Intermolecular Energy Transfer among Two Different Fluorophores and One Photoswitch. *Adv. Opt. Mater.* **2016,** *4* (5), 790.

(150) Zhu, L. L.; Li, X.; Zhang, Q.; Ma, X.; Li, M. H.; Zhang, H. C.; Luo, Z.; Agren, H.; Zhao, Y. L. Unimolecular Photoconversion of Multicolor Luminescence on Hierarchical Self-Assemblies. *J. Am. Chem. Soc.* **2013,** *135* (13), 5175.

(151) Kim, D.; Jeong, K.; Kwon, J. E.; Park, H.; Lee, S.; Kim, S.; Park, S. Y. Dual-color fluorescent nanoparticles showing perfect color-specific photoswitching for bioimaging and super-resolution microscopy. *Nat. Commun.* **2019,** *10*.

(152) Nakagawa, T.; Miyasaka, Y.; Yokoyama, Y. Photochromism of a spiro-functionalized diarylethene derivative: multi-colour fluorescence modulation with a photon-quantitative photocyclization reactivity. *Chem. Commun.* **2018,** *54* (26), 3207.

(153) Hudson, Z. M.; Lunn, D. J.; Winnik, M. A.; Manners, I. Colour-tunable fluorescent multiblock micelles. *Nat. Commun.* **2014,** *5*.

(154) Kim, H. J.; Whang, D. R.; Gierschner, J.; Lee, C. H.; Park, S. Y. High-Contrast Red-Green-Blue Tricolor Fluorescence Switching in Bicomponent Molecular Film. *Angew. Chem. Int. Ed.* **2015,** *54* (14), 4330.

(155) Xu, Z.; Gonzalez-Abradelo, D.; Li, J.; Strassert, C. A.; Ravoo, B. J.; Guo, D. S. Supramolecular color-tunable photoluminescent materials based on a chromophore cascade as security inks with dual encryption. *Mater. Chem. Front.* **2017,** *1* (9), 1847.

(156) Shen, X. Y.; Akbarzadeh, A.; Shi, C.; Pang, Z. Y.; Jin, Y.; Ge, M. Q. Preparation and characterization of photo-stimuli-responsive fibers based on lanthanide-activated phosphors and spiropyran dye. *J. Mater. Res. Technol.* **2021,** *13*, 1374.

(157) Zuo, M. Z.; Qian, W. R.; Li, T. H.; Hu, X. Y.; Jiang, J. L.; Wang, L. Y. Full-Color Tunable Fluorescent and Chemiluminescent Supramolecular Nanoparticles for Anti-counterfeiting Inks. *ACS Appl. Mater. Interfaces* **2018,** *10* (45), 39214.

(158) Jiang, K.; Sun, S.; Zhang, L.; Lu, Y.; Wu, A. G.; Cai, C. Z.; Lin, H. W. Red, Green, and Blue Luminescence by Carbon Dots: Full-Color Emission Tuning and Multicolor Cellular Imaging. *Angew. Chem. Int. Ed.* **2015,** *54* (18), 5360.

(159) Kwon, J. E.; Park, S.; Park, S. Y. Realizing Molecular Pixel System for Full-Color Fluorescence Reproduction: RGB-Emitting Molecular Mixture Free from Energy Transfer Crosstalk. *J. Am. Chem. Soc.* **2013,** *135* (30), 11239.

(160) Feng, H. T.; Xiong, J. B.; Zheng, Y. S.; Pan, B. A.; Zhang, C.; Wang, L.; Xie, Y. S. Multicolor Emissions by the Synergism of Intra/Intermolecular Slipped pi-pi Stackings of Tetraphenylethylene-DiBODIPY Conjugate. *Chem. Mater.* **2015,** *27* (22), 7812.

(161) Kim, J. H.; An, B. K.; Yoon, S. J.; Park, S. K.; Kwon, J. E.; Lim, C. K.; Park, S. Y. Highly Fluorescent and Color-Tunable Exciplex Emission from Poly(N-vinylcarbazole) Film Containing Nanostructured Supramolecular Acceptors. *Adv. Funct. Mater.* **2014,** *24* (19), 2746.

(162) Li, W.; Zhang, Y. M.; Zhang, T.; Zhang, W. R.; Li, M. J.; Zhang, S. X. A. Tunable RGB luminescence of a single molecule with high quantum yields through a rational design. *J. Mater. Chem. C* **2016,** *4* (7), 1527.

(163) Shiraishi, Y.; Ichimura, C.; Sumiya, S.; Hirai, T. Multicolor Fluorescence of a Styrylquinoline Dye Tuned by Metal Cations. *Chem. Eur. J.* **2011,** *17* (30), 8324.

(164) Teng, M. J.; Jia, X. R.; Chen, X. F.; Wei, Y. A Dipeptide-Based Multicolored-Switching Luminescent Solid Material: When Molecular Assemblies Meet Mechanochemical Reaction. *Angew. Chem. Int. Ed.* **2012,** *51* (26), 6398.

(165) Wang, J. W.; Wang, N.; Wu, G.; Wang, S. N.; Li, X. Y. Multicolor Emission from Non-conjugated Polymers Based on a Single Switchable Boron Chromophore. *Angew. Chem. Int. Ed.* **2019,** *58* (10), 3082.

(166) Wang, L.; Wang, K.; Zhang, H. Y.; Jiao, C. J.; Zou, B.; Ye, K. Q.; Zhang, H. Y.; Wang, Y. The facile realization of RGB luminescence based on one yellow emissive four-coordinate organoboron material. *Chem. Commun.* **2015,** *51* (36), 7701.

(167) Yuan, C. X.; Saito, S.; Camacho, C.; Irle, S.; Hisaki, I.; Yamaguchi, S. A pi-Conjugated System with Flexibility and Rigidity That Shows Environment-Dependent RGB Luminescence. *J. Am. Chem. Soc.* **2013,** *135* (24), 8842.

(168) Zhang, Z. Y.; Wu, Y. S.; Tang, K. C.; Chen, C. L.; Ho, J. W.; Su, J. H.; Tian, H.; Chou, P. T. Excited-State Conformational/Electronic Responses of Saddle-Shaped N,N '-Disubstituted-Dihydrodibenzo a,c phenazines: Wide-Tuning Emission from Red to Deep Blue and White Light Combination. *J. Am. Chem. Soc.* **2015,** *137* (26), 8509.

(169) Tsuchiya, S.; Sakai, K.; Kawano, K.; Nakane, Y.; Kikuchi, T.; Akutagawa, T. Color Changes of a Full-Color Emissive ESIPT Fluorophore in Response to Recognition of Certain Acids and Their Conjugate Base Anions. *Chem. Eur. J.* **2018,** *24* (22), 5868.

(170) Boole, G. *The Mathematical Analysis of Logic. Being an Essay Towards a Calculus of Deductive Reasoning*; Cambridge: Macmillan, Barclay, & Macmillan: London, **1847**.

(171) De Silva, A. P.; Gunaratne, H. Q. N.; McCoy, C. P. A MOLECULAR PHOTOIONIC AND GATE BASED ON FLUORESCENT SIGNALING. *Nature* **1993,** *364* (6432), 42.

(172) Ozlem, S.; Akkaya, E. U. Thinking Outside the Silicon Box: Molecular AND Logic As an Additional Layer of Selectivity in Singlet Oxygen Generation for Photodynamic Therapy. *J. Am. Chem. Soc.* **2009,** *131* (1), 48.

(173) Magri, D. C.; Fava, M. C.; Mallia, C. J. A sodium-enabled 'Pourbaix sensor': a three-input AND logic gate as a 'lab-on-a-molecule' for monitoring Na+, pH and pE. *Chem. Commun.* **2014,** *50* (8), 1009.

(174) Andréasson, J.; Terazono, Y.; Albinsson, B.; Moore, T. A.; Moore, A. L.; Gust, D. Molecular AND logic gate based on electric dichroism of a photochromic dihydroindolizine. *Angew. Chem. Int. Ed.* **2005,** *44* (46), 7591.

(175) Margulies, D.; Melman, G.; Shanzer, A. Fluorescein as a model molecular calculator with reset capability. *Nat. Mater.* **2005,** *4* (10), 768.

(176) Chen, S. J.; Yang, Y. H.; Wu, Y.; Tian, H.; Zhu, W. H. Multi-addressable photochromic terarylene containing benzo[b]thiophene-1,1-dioxide unit as ethene bridge: multifunctional molecular logic gates on unimolecular platform. *J. Mater. Chem.* **2012,** *22* (12), 5486.

(177) Jiang, X. J.; Ng, D. K. P. Sequential Logic Operations with a Molecular Keypad Lock with Four Inputs and Dual Fluorescence Outputs. *Angew. Chem. Int. Ed.* **2014,** *53* (39), 10481.

(178) Han, D.; Zhu, Z.; Wu, C. C.; Peng, L.; Zhou, L. J.; Gulbakan, B.; Zhu, G. Z.; Williams, K. R.; Tan, W. H. A Logical Molecular Circuit for Programmable and Autonomous Regulation of Protein Activity Using DNA Aptamer-Protein Interactions. *J. Am. Chem. Soc.* **2012,** *134* (51), 20797.

(179) Guz, N.; Fedotova, T. A.; Fratto, B. E.; Schlesinger, O.; Alfonta, L.; Kolpashchikov, D. M.; Katz, E. Bioelectronic Interface Connecting Reversible Logic Gates Based on Enzyme and DNA Reactions. *ChemPhysChem.* **2016,** *17* (14), 2247.

(180) Li, H. L.; Hong, W.; Dong, S. J.; Liu, Y. Q.; Wang, E. K. A Resettable and Reprogrammable DNA-Based Security System To Identify Multiple Users with Hierarchy. *Acs Nano* **2014,** *8* (3), 2796.

(181) Rout, B. A Miniaturized Therapeutic Chromophore for Multiple Metal Pollutant Sensing, Pathological Metal Diagnosis and Logical Computing. *Sci. Rep.* **2016,** *6*.

(182) Andréasson, J.; Straight, S. D.; Moore, T. A.; Moore, A. L.; Gust, D. Molecular all-photonic encoder-decoder. *J. Am. Chem. Soc.* **2008,** *130* (33), 11122.

(183) Budyka, M. F.; Li, V. M. Multifunctional Photonic Molecular Logic Gate Based On A Biphotochromic Dyad With Reduced Energy Transfer. *ChemPhysChem.* **2017,** *18* (2), 260.

(184) Andréasson, J.; Straight, S. D.; Bandyopadhyay, S.; Mitchell, R. H.; Moore, T. A.; Moore, A. L.; Gust, D. Molecular 2 : 1 digital multiplexer. *Angew. Chem. Int. Ed.* **2007,** *46* (6), 958.

(185) Elstner, M.; Axthelm, J.; Schiller, A. Sugar-based Molecular Computing by Material Implication. *Angew. Chem. Int. Ed.* **2014,** *53* (28), 7339.

(186) de Silva, A. P.; McClenaghan, N. D. Proof-of-principle of molecular-scale arithmetic. *J. Am. Chem. Soc.* **2000,** *122* (16), 3965.

(187) Andréasson, J.; Pischel, U. Storage and Processing of Information Using Molecules: The All-Photonic Approach with Simple and Multi-Photochromic Switches. *Isr. J. Chem.* **2013,** *53* (5), 236.

(188) de Silva, A. P.; Uchiyama, S. Molecular logic and computing. *Nat. Nanotechnol.* **2007,** *2* (7), 399.

(189) Andréasson, J.; Pischel, U. Smart molecules at work--mimicking advanced logic operations. *Chem. Soc. Rev.* **2010,** *39* (1), 174.

(190) Villada, J. D.; D'Vries, R. F.; Macías, M.; Zuluaga, F.; Chaur, M. N. Structural characterization of a fluorescein hydrazone molecular switch with application towards logic gates. *New J. Chem.* **2018,** *42* (22), 18050.

(191) Wu, Y.; Guo, Z.; Zhu, W.-H.; Wan, W.; Zhang, J.; Li, W.; Li, X.; Tian, H.; Li, A. D. Q. Photoswitching between black and colourless spectra exhibits resettable spatiotemporal logic. *Mater. Horiz.* **2016,** *3* (2), 124.

(192) Bälter, M.; Li, S. M.; Nilsson, J. R.; Andréasson, J.; Pischel, U. An All-Photonic Molecule-Based Parity Generator/Checker for Error Detection in Data Transmission. *Journal of the American Chemical Society* **2013,** *135* (28), 10230.

(193) Andréasson, J.; Kodis, G.; Terazono, Y.; Liddell, P. A.; Bandyopadhyay, S.; Mitchell, R. H.; Moore, T. A.; Moore, A. L.; Gust, D. Molecule-based photonically switched half-adder. *J. Am. Chem. Soc.* **2004,** *126* (49), 15926.

(194) Andréasson, J.; Straight, S. D.; Bandyopadhyay, S.; Mitchell, R. H.; Moore, T. A.; Moore, A. L.; Gust, D. A molecule-based 1 : 2 digital demultiplexer. *J. Phys. Chem. C* **2007,** *111* (38), 14274.

(195) Andréasson, J.; Straight, S. D.; Kodis, G.; Park, C. D.; Hambourger, M.; Gervaldo, M.; Albinsson, B.; Moore, T. A.; Moore, A. L.; Gust, D. All-photonic molecular half-adder. *J. Am. Chem. Soc.* **2006,** *128* (50), 16259.

(196) Andréasson, J.; Straight, S. D.; Moore, T. A.; Moore, A. L.; Gust, D. An All-Photonic Molecular Keypad Lock. *Chem. Eur. J.* **2009,** *15* (16), 3936.

(197) Straight, S. D.; Andréasson, J.; Kodis, G.; Bandyopadhyay, S.; Mitchell, R. H.; Moore, T. A.; Moore, A. L.; Gust, D. Molecular AND and INHIBIT gates based on control of porphyrin fluorescence by photochromes. *J. Am. Chem. Soc.* **2005,** *127* (26), 9403.